

May 2020

Modulating Matrix Metalloproteases and Inflammation in Huntington's Disease

Alejandro Lopez Ramirez
Dominican University of California

<https://doi.org/10.33015/dominican.edu/2020.BIO.04>

Survey: Let us know how this paper benefits you.

Recommended Citation

Lopez Ramirez, Alejandro, "Modulating Matrix Metalloproteases and Inflammation in Huntington's Disease" (2020). *Natural Sciences and Mathematics | Biological Sciences Master's Theses*. 10.

<https://doi.org/10.33015/dominican.edu/2020.BIO.04>

This Master's Thesis is brought to you for free and open access by the Department of Natural Sciences and Mathematics at Dominican Scholar. It has been accepted for inclusion in Natural Sciences and Mathematics | Biological Sciences Master's Theses by an authorized administrator of Dominican Scholar. For more information, please contact michael.pujals@dominican.edu.



This thesis, written under the direction of the candidate's thesis advisor and approved by the program chair, has been presented to and accepted by the Biological Sciences Program, at Dominican University of California, in partial fulfillment of the requirements for the degree of Master of Science in Biological Sciences.

Alejandro Lopez Ramirez
Candidate

Meredith Protas, PhD
Program Chair

Lisa M. Ellerby, PhD
First Reader

Kiowa Bower, PhD
Second Reader

Modulating Matrix Metalloproteases and Inflammation in Huntington's Disease

By

Alejandro Lopez-Ramirez

A culminating thesis submitted to the faculty of Dominican University of California in partial fulfillment of the requirements for the degree Master of Science in Biological Sciences

Dominican University of California

San Rafael, CA

May 2020

Copyright © 2020, by Alejandro Lopez Ramirez All Rights Reserved

Abstract

Huntington's disease (HD) is a rare and incurable autosomal neurodegenerative disease affecting 1-10 in every 100,000 people in the world. There is no cure for HD and treatments available alleviate certain symptoms for short periods of time. Evidence suggests that neuropathology of HD begins with the proteolysis of the mutated Huntingtin (mHTT) protein. A variety of proteases, like the matrix metalloproteases, cleave mHTT creating proteinaceous fragments that are thought to be neurotoxic. As these fragments increase in the brain, the damage to neurons also increases, leading to chronic inflammation due to hyper reactive microglia and astrocytes attempting to minimize and repair damages. There are many potential avenues to treat HD and, in this study, we provide insight on regulating proteolytic dysfunction with the systemic introduction of endogenous tissue inhibitor for metalloproteases-2 (TIMP2). In addition, we suppress inflammation in a selective manner with compound MW151 in order to attenuate the increasing levels of pro-inflammatory markers and reactive gliosis in HD.

Acknowledgements

The completion of this master's thesis project would not have been possible without the support, guidance, encouragement, and expertise from my mentors, Drs. Lisa M. Ellerby and Swati Naphade. I truly appreciate your help over these last two years.

I would like to thank the Ellerby Lab at the Buck institute for fostering and molding my scientific thinking. Everyone was extremely patient, kind, and knowledgeable. If it wasn't for all your helping hands, I would not have survived. A special thanks to Drs. Maria Sanchez and Barbara Bailus for teaching me how to dilute and write, again.

I am thankful for the support and leadership provided to us by Dr. Meredith Protas for spearheading the master's program and keeping us all on track even during the viral COVID-9 pandemic. I would like to thank Dr. Kristylea Ojeda for advising me and being there for me throughout my undergraduate and graduate time at Dominican. In addition, I would like to thank Drs. Georgia Woods and Kiowa Bower for providing a lot of wonderful feedback on my thesis.

Of course, I would like to thank my parents for always believing in me and sacrificing a lot of their own time, money, and dreams in order to keep me on track with my education.

Table of Contents

Abstract	iii
Acknowledgements	iv
List of Figures	vi
List of Tables	vii
List of Abbreviations	viii
Chapter 1	1
Abstract.....	1
Aims	2
Introduction	3
Methods	7
Results	14
Discussion.....	23
Chapter 2	25
Abstract.....	25
Aim	26
Introduction	27
Methods	30
Results	35
Discussion.....	55
References.....	58

List of Figures

Figure 1. Levels of the inactive pro-MMP2 and the active MMP2 isoform **Error! Bookmark not defined.**

Figure 2. Levels of TIMP2 are upregulated in R6/2 HD cortex and striatum when compared to WT controls..**Error! Bookmark not defined.**

Figure 3. Upregulation of TIMP2 in the HD striatum and an increase trend in TIMP2 in the HD the cortex compared to controls.....**Error! Bookmark not defined.**

Figure 4. MMP2 fluorometric assay demonstrates how the levels of the enzyme are increased in an HD mouse model.....**Error! Bookmark not defined.**

Figure 5. Western blot analysis of cortical and striatal lysates from WT mice, HD mice treated with PBS, and HD mice treated with the recombinant TIMP2.....**Error! Bookmark not defined.**

Figure 6. Western blot images of the levels of phosphorylated ERK and total ERK in the cortex and striatum of WT, PBS and TIMP2 treated R6/2 mice.**Error! Bookmark not defined.**

Figure 7. RNA-sequencing analysis, western blotting, and quantification of western blot from medium spiny neurons.**Error! Bookmark not defined.**

Figure 1. R6/2 Mouse Experiment layout.....**Error! Bookmark not defined.**

Figure 2. The weight of mice was recorded every Tuesday and Friday. Statistics shown from day 35 to day 101 are comparisons between WT and carrier mice (HD R6/2 mice). 35

Figure 3. Rotarod analysis was performed on weeks 5, 6, 9, and 12..... 37

Figure 4. Elevated plus maze results..... 39

Figure 5. Grip strength assay was performed twice, once for basal levels and the second round to determine grip force..... 41

Figure 6. Grip strength assay was performed only three times in the mice lifespan 42

Figure 7. Open field assay presenting movement in the horizontal and vertical plane. 44

Figure 8. Novel object recognition assay performed on the mice at 13 weeks of age..... 46

Figure 9. Short axis echocardiographs performed on 11-week-old mice **Error! Bookmark not defined.**-49

Figure 10. Life survival curve of the R6/2 mice treated with MW151 and saline. Mean lifespan of MW151. treated mice was 175 days and mean lifespan of saline treated mice was 163 days. 50

Figure 11. Metabolic cage data N=4 for each condition. Mice were single housed for the experiment.....	52
--	----

List of Tables

Table 1. List of Antibodies	7
-----------------------------------	---

List of Abbreviations

Ammonium persulfate (APS)
Bicinchoninic acid assay (BCA)
Brain-derived Neurotrophic Factor (BDNF)
Dulbecco's Modified Eagle Medium (DMEM)
Ethanol (EtOH)
Fibroblast growth factor (FGF)
Gamma Aminobutyric Acid (GABA)
Gamma Secretase Inhibitor IX (DAPT)
Green fluorescent protein (GFP)
Human Leukemia Inhibitory Factor (hLIF)
Huntingtin (HTT)
Huntingtin gene (*HTT*)
Huntington's disease (HD)
Induced pluripotent stem cells (iPSCs)
Intraperitoneal injection (IP)
Lithium dodecyl sulfate (LDS)
Mammalian protein extraction reagent (MPER)
Matrix Metalloproteinases (MMPs)
Medium spiny neurons (MSNs)
Membrane type 1- matrix metalloproteinase (MT1-MMP)
Mutant Huntingtin (mHTT)
Neural Proliferation Media (NPM)
Paraformaldehyde (PFA)
Penicillin-Streptomycin (P/S)
Phosphate buffered saline (PBS)
Poly-D-Lysine hydrobromide (PDL)
Polyglutamine (polyQ)
Polyvinylidene difluoride (PVDF)
Sodium dodecyl sulfate (SDS),
Tetramethylethylenediamine (TEMED)
Tissue inhibitor of metalloproteinases-2 (TIMP2)
Transforming growth factor beta (TGF- β)
Tris-buffered saline (TBS)
Tris-Buffered Saline with Tween (TBST)

Chapter 1

Abstract

Huntington's disease is caused by a polyglutamine (polyQ) repeat expansion located in the Huntingtin (HTT) protein. HD is known as an autosomal dominant neurodegenerative disorder, meaning that only one allele is required to contain the diseased gene on an autosomal chromosome. Evidence suggests that neuropathology of HD involves the proteolysis of the mHTT protein. Dysregulated matrix metalloproteinases (MMPs) lead to the proteolysis of mHTT, forming proteinaceous fragments that are thought to be neurotoxic, causing pathology in the striatum and cerebral cortex. MMP enzymatic activity is normally regulated by the endogenous tissue inhibitor of metalloproteinases (TIMPs). Published data in the R6/2 HD mouse model from our laboratory provide some evidence that MMPs are dysregulated. TIMP2 is the only inhibitor that regulates all the different forms of MMPs which can potentially be used to reduce MMP enzymatic activity and prevent mHTT proteolysis in the brain. HD isogenic induced pluripotent neural stem cells, medium spiny neurons and HD mouse models were used to evaluate expression levels of the MMPs and TIMPs. Analysis of mouse models of HD demonstrated an increase in TIMP2 levels in the striatum and cortex. In HD medium spiny neurons, the mRNA of MMPs was dysregulated when compared to controls. Further TIMP2 protein levels were reduced in the HD medium spiny neurons when compared to controls. Intraperitoneal injection of recombinant TIMP2 was administered to HD R6/2 mouse model and did not reduce MMP activity and related targets. We anticipate this negative result is due to dosage or delivery method.

Aims

Specific Aim 1: Previous studies have shown highly dysregulated matrix metalloproteinases (MMPs) causing fragmentation of the N-terminal region in HD resulting in shorter toxic fragments. The specific location of MMPs in stem cells will be investigated. Understanding MMP proteolytic activity will be studied using western blots, immunocytochemistry, and RT-PCR in a human stem cell model of HD. The isogenic HD and control corrected C116 induced pluripotent stem cell (iPSC) model will be differentiated from standard protocol into neural stem cells and further differentiated to medium spiny neurons, microglia, and astrocytes.

Specific Aim 2: Endogenous tissue inhibitors of metalloproteinases (TIMPs) naturally occur in the body to regulate MMPs. It is known that TIMP-2 assists the central nervous system (CNS) by preventing early cellular apoptosis and anti-inflammatory roles which can attenuate the inflammatory response in HD brains. We will systemically introduce recombinant TIMP-2 protein and adeno-associated viral TIMP-2 into HD R6/2 transgenic mice. Upregulation of the endogenous inhibitor affects behavior and motor skills, in which we will observe and analyze with a wide variety of behavioral studies. Biochemical assays will elucidate uptake of TIMP-2.

Introduction

Huntington's disease is an autosomal dominant genetic disease affecting 10 persons in every 100,000 (Becker et al., 2010). Disease progression is directly related to CAG repeat length found in exon 1 of the Huntingtin gene (*HTT*). Disease symptoms usually occurs between the ages of 40 and 50. The age of onset is directly correlated to the length of the CAG expansion in exon 1. Longer repeats can result in juvenile onset whereby symptoms present during childhood and patients usually die within the next 10-15 years (Saudou & Humbert, 2016). It is thought that the polyQ-expanded protein has altered susceptibility to proteolytic cleavage and misfolding, which results in neurotoxic fragments derived from the mutant huntingtin protein (Gafni et al., 2012; Hermel et al., 2004; Landles et al., 2010; Miller et al., 2010; Schilling et al., 2006; Tanaka et al., 2006). These fragments have been discovered in affected post-mortem human HD tissue, but also, importantly, in presymptomatic HD mouse models, suggesting that the misfolding and proteolysis of mHTT is required for disease progression (Gafni & Ellerby, 2002; Gafni et al., 2012; Hermel et al., 2004; Landles et al., 2010; Miller et al., 2010; Schilling et al., 2006; Tanaka et al., 2006). Furthermore, the proteolysis of mHTT leads to the loss of medium spiny neurons (MSNs) that are found in the striatum and neural atrophy includes the cerebral cortex (Lieberman, Shakkottai, & Albin, 2019). Inhibiting proteolytic cleavage of mHTT has been shown to be neuroprotectant *in vitro* and *in vivo* by rescuing the loss of medium spiny neurons and ultimately restoring motor function and some cognitive function (Crotti & Glass, 2015; Gafni et al., 2012; Graham et al., 2006).

A wide variety of caspases and calpains are known proteolytic enzymes that can cleave HTT and in turn increase the number of toxic fragments which are further cleaved to generate smaller fragments at the N-terminus (Gafni & Ellerby, 2002; Gafni et al., 2012; Hermel et al.,

2004; Landles et al., 2010; Schilling et al., 2006; Tanaka et al., 2006). *Miller et al.* screened 514 known proteases for their ability to modulate the cleavage of mHTT in the N-terminal region of HTT, a fragment generated in the amino acid region between 100 to 167 (Miller et al., 2010). Cellular lysates from the siRNA screen were analyzed by western blot to determine which proteases reduced the amount of the mutant HTT toxic fragment. Results show that of the 514 proteases, 11 of them reduced the levels of the mHTT fragment formation. Given these 11 proteases were found to modulate the proteolysis of mHTT, the team proceeded to validate with siRNA how these 11 proteases affected HD cellular toxicity. As predicted, the reduction of these proteases reduced HD cellular toxicity. Remarkably, 3 of those mHTT proteolysis modifiers fall into the matrix metalloproteinase (MMP) family, specifically MMP10, 14, and 23B and reduction of this family of enzymes reduced HTT proteolysis and toxicity (Miller et al., 2010).

MMPs are Ca^{2+} dependent, zinc-containing proteolytic enzymes. Currently, there are 25 known MMPs in the human body and they are further categorized as matrilysins, collagenases, gelatinases, stromelysins, and membrane-type MMPs. Matrix metalloproteinases are secreted into the extracellular matrix as zymogens (Pro-MMPs) and then later activated by most endogenous tissue inhibitors of metalloproteases (TIMPs), proteases, or radicals (Li, Tay, & Yiu, 2020; Naphade, Embusch, Madushani, Ring, & Ellerby, 2017; Rivera, 2019; Rivera, Garcia-Gonzalez, Khrestchatisky, & Baranger, 2019). MMPs physiological function include cytoskeletal rearrangement, wound repair, and general repair of the matrix. In the human body, MMPs are regulated by TIMPs. The TIMP family is made up of four members, TIMPs 1 through 4, and they bind to the MMPs catalytic Zn^{2+} domain. TIMPs not only serve as inhibitors but can also serve as catalyzing agents. For example, TIMP2 will aid the docking of pro-MMP2 to the cell

surface where the MMP2 is then activated by membrane type 1- matrix metalloproteinase (MT1-MMP, MMP14) (Egeblad & Werb, 2002).

In examining HD cell and mouse models, *Naphade et al.*, discovered that MMP10 and MMP14 were dysregulated and this correlated with the levels of TGF- β in isogenic HD neural stem cells derived from patient HD iPSCs (Naphade et al., 2017). When MMP10 and 14 were knocked down via siRNA, there was a significant reduction in caspase-3/7 activity, indicating less cell death in a striatal model of HD. Further evidence that MMPs are involved in pathogenesis stems from *Drosophila* models of HD, whereby controlling the dysregulation of MMPs can restore motor function (Miller et al., 2010). Taken together these data support the possibility that therapies aimed at regulating MMPs can reduce the amount of mHTT proteolysis and reduce the loss of medium spiny neurons in the striatum.

Thus far, studies aimed at curbing proteolytic cleavage and the formation of toxic fragments, have mostly relied on genetic based manipulations of MMPs and TIMPs, yet it remains to be determined whether pharmacological interventions, that target MMP activity, are effective at mitigating disease progression. Pharmacological inhibitors of MMPs have been described, but most broadly inhibit all MMPs resulting in harmful side-effects like musculoskeletal syndrome, preventing their therapeutic usefulness. *Becker et al.*, devised a new variety of MMP hydroxamate-based inhibitors, 19v, 19w, and 9j, which allosterically inhibit the MMPs 2, 9, and 13 meanwhile sparing MMP1 (Becker et al., 2010). These compounds were previously used by *Madushani, L. K.*, and showed that 9j was a top candidate in MMP inhibition, specifically the gelatinases MMP2 and 9 (Madushani, 2018). Overall, this data provided further evidence that inhibiting MMPs can confer neuroprotection in HD cellular models.

Here we investigate MMP and TIMP interactions in an isogenic HD neural stem cell and medium spiny neuron model derived from HD patient iPSCs as well as in two HD transgenic mouse models. While some published studies have demonstrated increases or decreases in cellular levels of MMPs and TIMPs, they have not focused their attention on potential changes in other proteins that function in the MMP pathways. Furthermore, such studies have examined changes that occur in neural stem cells but not in differentiated cells. To better understand the nuance of how MMP pathways becomes dysregulated in HD, and the cell types that are subject to this dysregulation, we have examined MMPs in neural stem cells, medium spiny neurons, and mouse models of HD. In addition, we systemically introduced recombinant or viral TIMP2 into an R6/2 HD mouse model in order to rescue motor and cognitive functions. This study provides further studies on the effects of the use of TIMP2 in HD stem cell and mouse models.

Methods

Bicinchoninic Acid Assays and Western Blot

Neural stem cell lines were lysed with mammalian protein extraction reagent (MPER) (10 mL, Thermo Fisher Scientific, 78501) and complete protease inhibitors (1 tablet/10 mL, Roche, 11836170001). Neural stem cell extracts were processed further via sonification using 5 seconds of pulsing, 5 seconds of rest for 5 rounds at 40 mA. Samples were then spun down at 14,000 rpms at 4°C for 20 minutes. Protein concentration was quantified with a bicinchoninic acid assay (BCA). Protein was loaded (15 µg) onto a 4-12% bis-tris gel along with dithiothreitol (1 µL) and 4X Lithium dodecyl sulfate (LDS) Nu-Page buffer (6 µL, Invitrogen, NP0007). Proteins were boiled at 95°C for 10 minutes. Gels were run at 200V for 1 hour. They were then transferred over to a polyvinylidene difluoride (PVDF) membrane overnight at 20V at 4°C. Membranes were then blocked with 5% non-fat milk for 1 hour. Primary antibodies were added to the membrane and probed overnight at 4°C. Washes (3X) with 1X Tris-buffered saline with tween (TBST) were performed. Secondary antibody was added and kept on for 1 hour at room temperature. Membranes were then washed (3X) off once again in 1X TBST and imaged with Pierce enhanced chemiluminescence reagents (700 µL, Thermo Fisher Scientific, 32106).

List of Antibodies Used in Western Blots

Table 1. List of Antibodies

Name	Species Host	Company	Product Number	Dilution
MMP3/10	Mouse	Santa Cruz Biotechnology	SC-374029	1:200
MMP9	Rabbit	Santa Cruz Biotechnology	SC-10737	1:200

MMP2	Rabbit	Abcam	Ab53771	1:100
TIMP2	Rabbit	Cell Signaling Technology	CST-5738	1:400
PolyQ 1C2	Mouse	Millipore	MAB1574	1:400
GFAP	Rabbit	Sigma	G4546	1:500
MMP3	Rabbit	Cell Signaling Technology	SC-6839	1:250
β -Actin	Mouse	Millipore-Sigma	A5441	1:2000
DARPP-32	Mouse	Santa Cruz Biotechnology	SC-29111	1:100
GFP	Mouse	Santa Cruz Biotechnology	SC-9996	1:100
ERK1/2	Rabbit	Cell Signaling Technology	CST-4370	1:500
p-ERK1/2	Rabbit	Cell Signaling Technology	CST-4695	1:500
HTT	Mouse	Millipore-Sigma	MAB2166	1:250
Vinculin	Mouse	Sigma Aldrich	V9131	1:2000

Cell Cultures

Neural stem cells were generated from human isogenic C116 and HD induced pluripotent stem cells (iPSCs) using STEMdiff Neural Induction Medium. Matrigel (1 mL, 50 μ g, Corning, CB-40234) was coated in Corning 6 cm plates overnight (An et al., 2012; Naphade et al., 2017; Ring et al., 2015). NSCs were cultured in Neural Proliferation Medium (NPM) (3 mL, Gibco, 21103049) with fibroblast growth factor (FGF) (25 ng/mL, Peprotech, 10025) and activin-A (25 ng/mL, Peprotech, AF-120-14E) in a humidified incubator (37°C and 5% CO₂). Preparation of the NPM required 1X B27 supplement (1 mL, Gibco, A3582801), human Leukemia Inhibitory Factor (hLIF) (10ng/mL, Peprotech, 300-05), L-Glutamine (5 mL, Gibco, 350550061),

Penicillin-Streptomycin (P/S) (5 mL, Invitrogen, 15140122), and Neurobasal Medium (500 mL, Gibco, 21103049). Media was changed every other day and replaced with new media (3 mL).

Medium Spiny Neuron Differentiation

HD and C116 Activin A (25 ng/mL, Peprotech, AF-120-14E) NSCs were used to prepare MSNs. Nunc 6-well plates were treated with poly-D-lysine hydrobromide (PDL) (1 mL, 100 μ g/mL by Sigma Aldrich, P6407) and incubated (37°C and 5% CO₂) overnight. Plates were washed once (1mL, Corning cell culture grade water, 25-055-CVC) and left to air dry for 1 hour inside the culture hood. Next, the plate was treated with Matrigel (1 mL, 50 μ g, Corning, CB-40234) overnight in incubator. Matrigel was replaced with Synaptojuice A media (2 mL) prior to seeding neural stem cells (1x10⁶ per well)(Kemp et al., 2016). Synaptojuice A was prepared with 10X Synaptojuice A supplement (5 mL), advanced DMEM/F12 media (44.1 mL, Gibco, 12634010), P/S (450 μ L, Invitrogen, 15140122), and 100X Glutamax (450 μ L, Invitrogen, 35050079). Synaptojuice A supplement contains advanced DMEM/F12 media (38 mL), MACS NeuroBrew-21 (10 mL, MACS Miltenyi Biotec, 130-093-566), PD0332991 (100 μ L, 20 μ M, Tocris Bioscience, 4786), DAPT (100 μ L, 100 μ M, Tocris Bioscience, 2634), human BDNF (50 μ L, 100 ng/mL, MACS Miltenyi Biotec, 130-096-286), LM22A4 (25 μ L, 5 μ M, Tocris Biotec, 4607), Forskolin (500 μ L, 100 μ M, Tocris Bioscience, 1099), CHIR 99021 (250 μ L, 30 μ M, Tocris Bioscience, 1099), GABA (500 μ L, 3 mM, Tocris Bioscience, 0344), CaCl₂ (370 μ L, 1.8 mM, Tocris Bioscience, 3148), ascorbic acid (100 μ L, 2 mM, Tocris Bioscience, 4055). Media is passed through a 0.22 μ m filter. Cells were treated with Synaptojuice A (2 mL) for 7 days, performing half media changes every other day. On day 8, full media changes were completed and then treated with synaptojuice B (2 mL) for the next 7 days. Synaptojuice B was prepared

with 10X synaptojuice B (5 mL) supplement and Basal Media (45 mL). Basal media contains advanced DMEM/F12 media (22.5 mL), P/S (450 μ L, Invitrogen, 15140122), and 100X Glutamax (450 μ L, Invitrogen, 35050079) and Neurobasal A Media (22.5 mL, Gibco, 10888022), P/S (450 μ L, Invitrogen, 15140122), and 100X Glutamax (450 μ L, Invitrogen, 35050079). Synaptojuice B supplement contains advanced DMEM/F12 media (19.7 mL), Neurobasal A media (19.7 mL), MACS NeuroBrew-21 (10 mL, MACS Miltenyi Biotec, 130-093-566), PD0332991 (100 μ L, 20 μ M, Tocris Bioscience, 4786), human BDNF (50 μ L, 100 ng/mL, MACS Miltenyi Biotec, 130-096-286), LM22A4 (25 μ L, 5 μ M, Tocris Biotec, 4607), CHIR 99021 (250 μ L, 30 μ M, Tocris Bioscience, 1099), GABA (500 μ L, 3 mM, Tocris Bioscience, 0344), CaCl₂ (370 μ L, 1.8 mM, Tocris Bioscience, 3148), ascorbic acid (100 μ L, 2 mM, Tocris Bioscience, 4055). Synaptojuice B media is filtered through a 0.22 μ m filter. Cells were treated with Synaptojuice B (2 mL) for 7 days and half media changes were performed until day 14. Cells were harvested in mammalian protein extracting reagent (150 μ L, Thermo Fisher Scientific, 78501) mixed with a protease inhibitor cocktail (1 tablet/10 mL, Roche, 11836170001).

Gelatin Zymography

C116 and HD neural stem cells were harvested in lysis buffer (50 mM Tris-HCL, pH 7.6), 150 mM NaCl, 5 mM CaCl₂, 0.05% Brij-35, 1% Triton X-100, 0.02% NaN₃), and sonicated as described above. For each sample, 500 μ g of sonicated cell lysate was suspended in 500 μ L of lysis buffer and 50 μ g of Gelatin Sepharose 4B beads (GE healthcare) and placed on rotator for 1 hour at 4°C for MMP binding. Suspensions were centrifuged, supernatant was removed, and affinity-bound MMPs were eluted by resuspending the bead complexes in 100 μ L elution buffer (10% DMSO in PBS). 20 μ g of elute (with 4X LDS sample buffer) was then loaded on a 8%

zymogram gel containing 0.1% gelatin (Resolving gel: 1.5 M Tris-HCl, pH 8.8), 0.4% sodium dodecyl sulfate (SDS), ddH₂O, 40% acrylamide/bis-acrylamide, tetramethylethylenediamine (TEMED), 10% ammonium persulfate (APS), and 0.1% gelatin. Stacking gel: 1.0 M Tris-HCl (pH 6.8), ddH₂O, 40% acrylamide/bis-acrylamide, TEMED, 10% APS). Zymogram gels were run in 1X Tris-Glycine SDS buffer under non-reducing conditions at 150 V for 1 hour. Gels were then washed with renaturation buffer (2.5% Triton X-100 in ddH₂O) for 40 minutes at 25°C, briefly rinsed with ddH₂O, and incubated in 50 mL of incubation buffer (50 mM Tris HCl, 0.15 M NaCl, 10 mM CaCl₂) for 20-72 hour at 37°C. Finally, gels were briefly washed with ddH₂O, stained with 0.05% Coomassie Brilliant Blue solution for 1 hour, and de-stained for 1 hour at room temperature. Images were scanned using an Epson Scanner.

For conditioned media, fresh medium was added to near-confluent cultures and the media was harvested after 3 days of incubation at 37°C and 5% CO₂. 500 µL of conditioned media was loaded onto Amicon Ultra-0.5 Centrifugal Filter Devices (EMD Millipore, UFC501008) with a molecular weight cut-off of 10 kDa. Conditioned media was concentrated to 20 µL by centrifuging the devices at 14,000 x g for 30 minutes. Concentrated media was recovered by turning the devices upside down in clean tubes and centrifuging the tubes at 1000 x g for 2 minutes. 20 µg of elute (with 4X LDS sample buffer) was then loaded on an 8% zymogram gel containing 0.1% gelatin, and gelatin zymography was performed as described above.

Immunocytochemistry

Cells were cultured in an 8 well chamber slide and fixed with 4% paraformaldehyde (PFA) for 15 minutes in room temperature. After fixing, the 8 wells were washed 3X with 1X PBS. The cells were then incubated with primary antibody at 4°C overnight. After, the slides were washed 3X with PBS and then blocked with secondary antibody and incubated for 2 hours

at room temperature. Three washes were performed once again with PBS. Slides were then mounted with a coverslip and adhered with Prolong Gold for 24 hours at room temperature in the dark.

Immunohistochemistry

All mouse tissue was sectioned into slices, 5 μm thick, and then paraffin embedded. Once required, the paraffin was removed using one round for 5 minutes of each solution containing xylene, 100% ethanol (EtOH), 95% EtOH, 80% EtOH, 70% EtOH, & 50% EtOH. Rinsed slides with distilled water and then washed in tris-buffered saline (TBS) (100 mM) for 10 minutes on a rotating platform (50 rpm). Antigen retrieval was performed by placing slides in a coplin jar containing citrate buffer (pH 6.0, 10 mM) for 5 minutes in a microwave (400 W). Citrate buffer was left to cool for 20 minutes at room temperature for 20 minutes. Remove citrate buffer and rinse slides off with tris-buffered saline for 10 minutes on a rotating platform turning at 50 rpm. Slides were thoroughly dried and using a liquid pap-pen (Sigma Aldrich, Z377821) created box borders around the tissue sections. Sections were then blocked for an hour in blocking serum (200 μL , 1% bovine serum albumin, 5% donkey serum, and TBS). In addition to the blocking serum, we added goat anti-mouse IgG (Jackson ImmunoResearch, 115-005-003). After blocking, tissue sections were washed three times for 10 minutes with 1X TBS. Primary antibodies were added at desired concentrations in blocking buffer and left overnight at 4°C in humid chambers. Next day, sections were washed three times for 10 minutes with 1X TBS. Secondary antibody was added and left on for an hour in a dark humid chamber. Antibody was washed off three times for 10 minutes with 1X TBS. The slide cover was mounted on with ProLong Gold (200 μL , Invitrogen, P36930) and left overnight to cure. Imaging took place in our Biotek automated incubator.

Systemic Introduction of Recombinant or Viral TIMP2

Introduction of recombinant TIMP2 (R&D Systems, 6304-TM-010, 10 μ g) occurred via intraperitoneal injection (IP) three times a week. TIMP2 was diluted down to a stock concentration of 0.025 μ g/ μ l. We injected each mouse at 50 μ g/kg for 3 weeks. Mice were sacrificed two hours after final injection was given.

Viral TIMP2 and control green fluorescent protein (GFP) (SignaGen, SL100861, 3.22 E+13 VG/ml) was injected in mice at a concentration of 1.5 E+11 VG/ml (Castellano et al., 2017) One-time injection via tail vein was performed. Harvesting of mice occurred 6 weeks post-injection.

Fluorometric Assay

Brain tissues of mice were homogenized in lysis buffer (50 mM Tris-HCl, 150 mM NaCl, 5 mM CaCl₂, 0.05% Brij-35, 1% TritonX-100, 0.02% NaN₃), sonicated 3X for 30 seconds with 30 seconds of rest at 40% amplitude. Centrifuged samples at 14,000 rpm for 20 minutes at 4°C. BCA assay (Pierce) was performed to determine the protein concentration. 150 μ g of protein, 7.5 μ g of NNGH, 4 μ M of fluorogenic substrate, Mac-Pro-Leu-Ala-Nva-Dap (Dnp)-Ala-Arg-NH₂ (Enzo Labs), and assay buffer (50 mM HEPES, 10 mM CaCl₂, 0.05% Brij-35, pH 7.5) was loaded onto a 96 well black-bottom plate. Substrate fluorescence intensity was measured (Ex: 485 nm and Em: 530 nm) at 37°C by VictorX plate reader (Perkin Elmer). The enzymatic activity was normalized to protein concentration of each sample. Fluorescence reading were provided by Workout Plus software. Fluorescent measurements of the TIMP2 induced lysates were compared to the addition of NNGH, a broad spectrum MMP inhibitor, to measure the overall activity of MMP2 and MMP9.

Results

Activated MMP2 in Neural Stem Cells is Regulated with TGF- β

Gelatin zymography is used to identify gelatinases, like MMP2, in culture media, cell extracts, and tissue extracts. The SDS gels used are co-polymerized with gelatin. In order to maintain enzymatic activity, samples are electrophoresed under nonreducing conditions and then later partially re-activated using a calcium-containing renaturing buffer. Staining the gel with Coomassie Blue allows us to visualize the enzymes as we can see transparent bands in a blue background. These transparent bands are located at the appropriate molecular weight as confirmed with the blood standard molecular weight shown in the far left in Figure 1. Although there seems to be high activity originating from non-active pro-MMP2, under physiological conditions the enzyme is not actively degrading gelatin. The main reason for the activity is due to the SDS in the gel as it denatures the entire enzyme. The pro-domain that blocks binding to the catalytic zinc domain is now permanently inactive and the enzyme begins degrading surrounding gelatin.

Treatment of cells with transforming growth factor beta (TGF- β) is known to be neuroprotective and we have recently demonstrated this growth factor modulates the levels of TIMPs and MMPs (Naphade et al., 2017). Treatment with TGF- β increases the amount of TIMP1 which suppresses the amount dysregulated levels MMP-2, -3 and -10 that are actively cleaving the full length mHTT. To further examine this, we added 10 ng/ μ L of TGF- β to human isogenic corrected (C116) and HD neural stem cells for 72 hours and carried out gelatin zymography. Consistent with the activation of MMPs in HD, HD NSCs have higher levels of the activated MMP2 isoform when compared to the control C116 NSCs (Figure 1). The addition of TGF- β does not appear to reduce the activate form of MMP2 found just below the 72 kDa band

(Figure 1). Further studies using increasing amounts of TGF- β will determine if this reduces the amounts of the gelatinase activity and reduce the amount mHTT fragments from forming.

Gelatin Zymography of Huntington's Diseased Cells & Corrected Cells

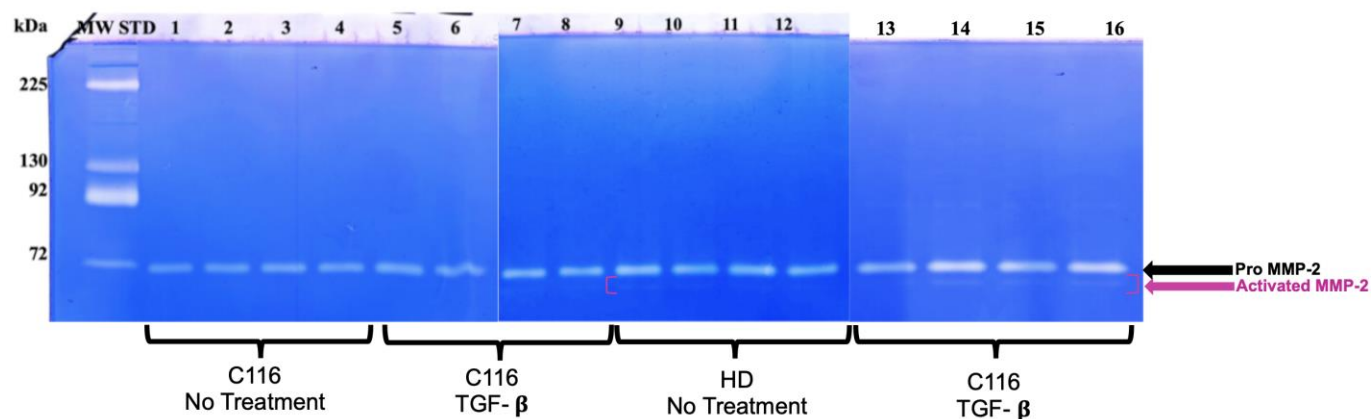


Figure 1. Levels of the inactive pro-MMP2 and the active MMP2 isoform. The molecular weight is derived from human peripheral blood which classically shows four main gelatinolytic bands corresponding to the zymogenic forms of pro-MMP2 (72 kDa), monomeric pro-MMP9 (92 kDa), dimer pro-MMP9 (130 kDa), and pro-MMP9 multimeres (225 kDa). Lanes 1-4 contain corrected C116 neural stem cell lysates without TGF- β treatment. Lanes 5-8 are the C116 neural stem cell lysates after treatment with TGF- β . Beginning at lane 9 we can begin to see active MMP2 below the pro-MMP2 isoform, as indicated by the pink brackets. Lanes 9-12 contain HD neural stem cells without treatment. Lanes 13-16 contain HD neural stem cell lysates with TGF- β treatment. Faint bands of the active MMP2 isoform can be seen within the corrected cells lines with and without TGF- β treatment but are far more apparent in both the HD lines with and without treatment.

TIMP2 is Upregulated in the Cortex of R6/2 HD Mice

The levels of TIMP family members has not been evaluated in HD mouse models. To evaluate TIMP levels, we used two well-characterized mouse models of HD. The R6/2 fragment model expresses the exon-1 derived polyQ-expanded protein fragment of HTT (Davies et al., 1997; Mangiarini et al., 1996). The full-length knock in mouse model, HD-zQ175, expresses full-length polyQ expanded HTT with 175 polyQ repeats. As shown in Figure 2, we found an increase in TIMP2 levels in the R6/2 HD in the cortex. The increase of TIMP2 levels most likely occurs to compensate for the increased levels of MMPs.

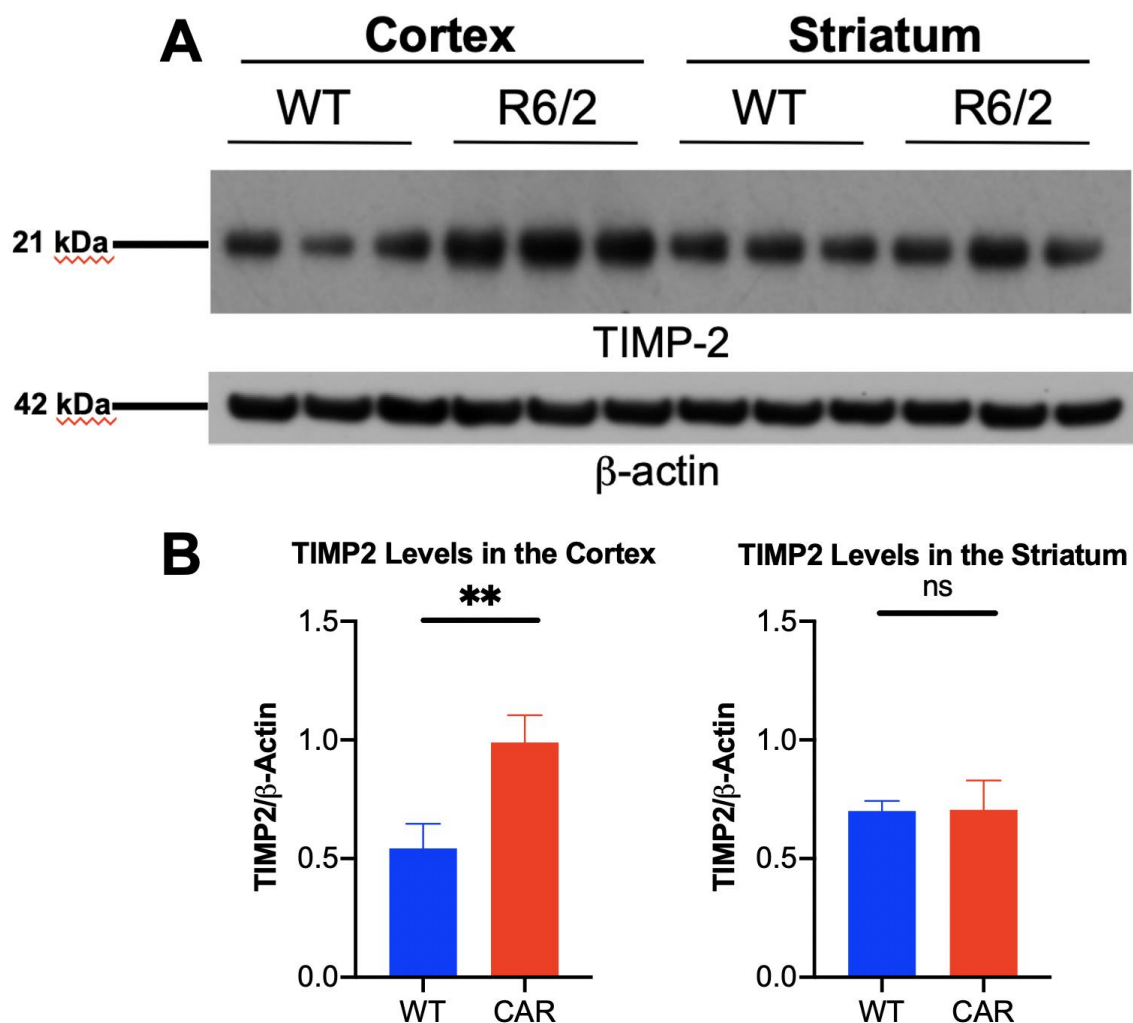


Figure 2. Levels of TIMP2 are upregulated in R6/2 HD cortex and striatum when compared to WT controls. A) Western blot was performed on 4-month-old mice probing for TIMP2 and β -actin levels. B) Quantification of the western blot was carried out using ImageQuant software. A significant increase in TIMP2 levels found in the cortex while there is no change in TIMP2 levels in the striatum of HD mice compared to controls (*t*-Test).

TIMP2 Expression is Upregulated in the Striatum of zQ175 Mice

Further evaluation of the TIMP2 levels was performed using western blot analysis in the zQ175 mice. The zQ175 is a knock in mouse model, replacing the mouse *HTT* gene with the full length human *mHTT* containing a 175 CAG tract in exon 1. As shown in Figure 3A,C, we found an increase of TIMP2 levels in the striatum of the zQ175 mice when compared to littermate controls (WT). There was also an increase in the levels of TIMP2 in the zQ175 cortex but it did

not reach statistical significance when compared to WT (Figure 3A,B). These results may suggest that the upregulation of TIMP2 in HD occurs to regulate MMPs which are increased in activity in HD mouse models, postmortem tissue and blood (Crotti & Glass, 2015; Miller et al., 2010; Rocha, Ribeiro, Furr-Stimming, & Teixeira, 2016).

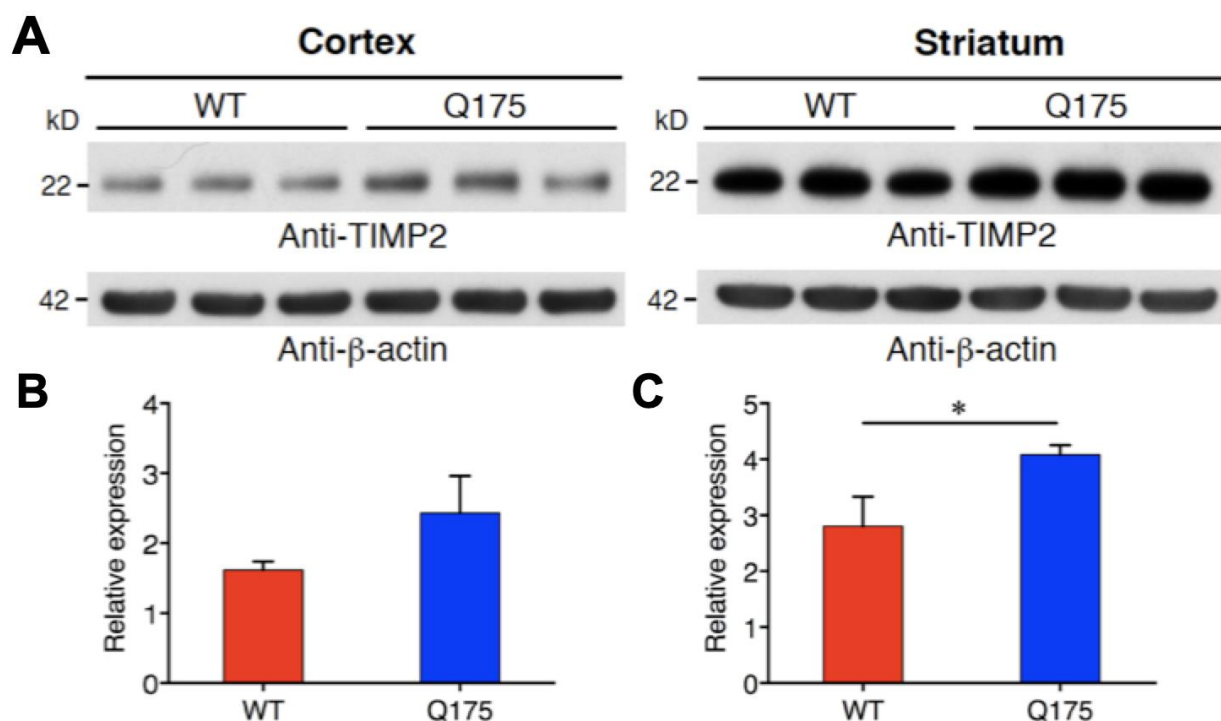


Figure 3. Upregulation of TIMP2 in the HD striatum and an increase trend in TIMP2 in the HD the cortex compared to controls. A) Western blot from cortical and striatal lysates acquired from 12-month-old α Q175 and control mice. Quantified with ImageQuant. B and C) Quantification of western blots. There was a significant increase in TIMP2 in the striatum of Q175 mice while the levels of TIMP2 in the cortex were not statistically significant.

Evaluating TIMP2 with MMP Fluorometric Assay

We established an MMP assay to confirm alterations in MMP activity in mouse models of HD and to evaluate if treatment of HD mice with TIMP2 lowered MMP activity. We used the MMP2 fluorometric assays to determine the efficacy of our MMP inhibitor. The assay uses a quenched fluorogenic peptide (Mca-Pro-Leu-Gly-Leu-Dpa-Ala-Arg-NH) in which the Mca fluorophore is quenched by the Dpa group. In the presence of active MMP2, the enzyme will cleave between the Gly-Leu groups resulting in the Mca emitting fluorescence. The assay was

run on three samples in triplicates, twice on the plate. One row contained the sample without NNGH inhibitor and the second row with the NNGH inhibitor. The NNGH inhibitor is provided in the kit to determine how much of the change in fluorescence signal is due to actual MMP activity. The substrate can react with other non MMP enzymes.

Confirmation of dysregulated MMP2 in neural stem cells and TIMP2 in HD mouse models led us to treat HD mice with recombinant TIMP2 using IP injection at 0.05 $\mu\text{g}/\text{kg}$ for 17 days. Once the dosing was completed, the mice brains were harvested and ran on the aforementioned fluorometric assay. In Figure 4, the brain stem and cerebellum of the non-injected, PBS, and TIMP2 treated mice were processed and placed in the fluorometric assay to determine the efficacy of TIMP2 in inhibiting MMP2 activity. In the cerebellum, the levels of MMP2 are similar in the HD mice compared to controls (Figure 4A). In the brain stem, we detect a small increase in MMP2 activity in R6/2 compared to WT but it does not reach statistical significance. In the striatum, there is an increase in MMP2 activity in R6/2 mice when compared to controls (Figure 4A) consistent with MMP2 are increasing in the HD mouse model. We did not find a decrease in MMP2 activity in the mice treated with recombinant TIMP2 (Figure 4). The levels are increased although not statistically significant.

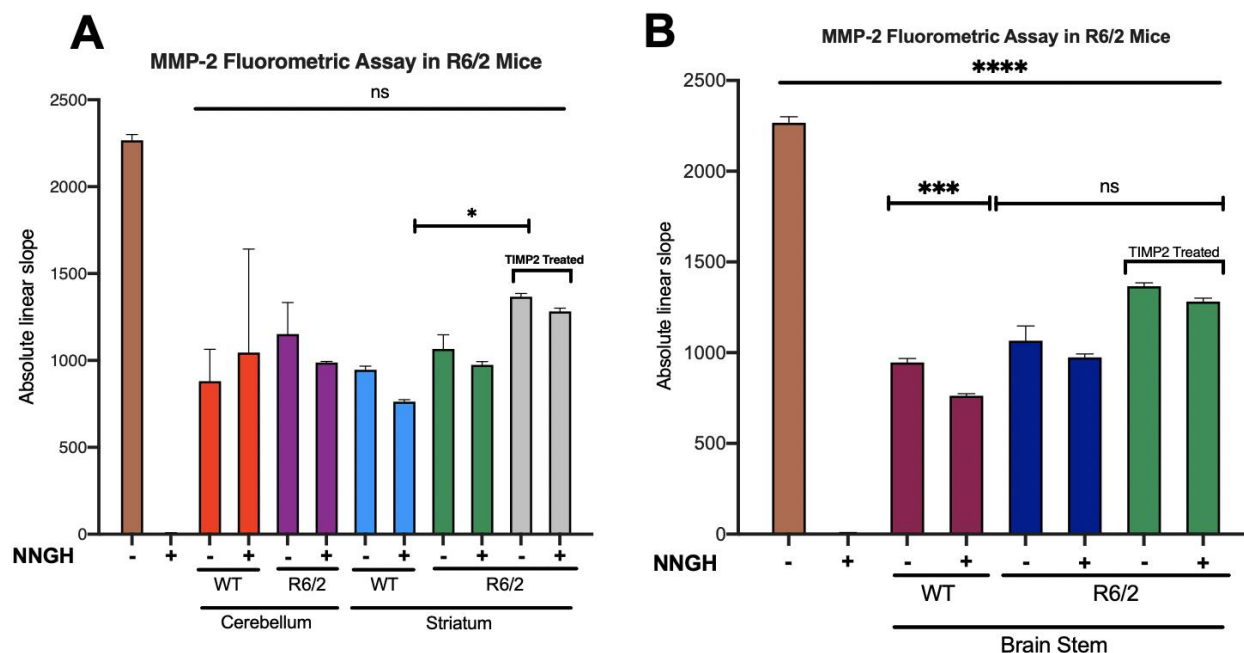


Figure 4. MMP2 fluorometric assay demonstrates how the levels of the enzyme are increased in an HD mouse model. Lysates acquired from 3-month-old mice. A) First bar graph (brown) does not contain any inhibitors, only MMP2 enzymes and buffers. Second bar (NNGH inhibitor) contained only the inhibitor and no MMP2 enzymes. Cerebellum samples from the WT and HD mice were used as positive controls from a previous MMP2 fluorometric assay. Common levels of MMP2 activity are seen in the three sets of brain stems. Addition of TIMP2 did not reduce the levels of MMP2 in the striatum. B) First bar graph (brown) does not contain any inhibitors, only MMP2 enzymes and buffers. Second bar (NNGH inhibitor) contained only the inhibitor and no MMP2 enzymes. WT mice and HD mice without recombinant TIMP2 treatment were used as controls. Far right bar graph contains a treated mouse. No significant changes were observed in two brain regions of the R6/2 mouse.

IP Injection of Recombinant TIMP2 and analysis of TIMP2 in the Cortex and Striatum

From the fluorometric assay, it is not likely that TIMP2 was delivered to the brain based on the increased level of that MMP2 activity. To further confirm this, we ran a western blot analysis of TIMP2 levels in the brain. We processed the cortex and striatum and ran them on a western blot (Figure 5A) and then quantified the bands with ImageQuant software. We detected lower levels of TIMP2 in the striatum of TIMP2 injected R6/2 mice as shown in Figure 5. We based our injection protocol on published studies evaluating the effect of TIMP2 on aging in the brain (Castellano et al., 2017). More studies are needed to understand our negative results.

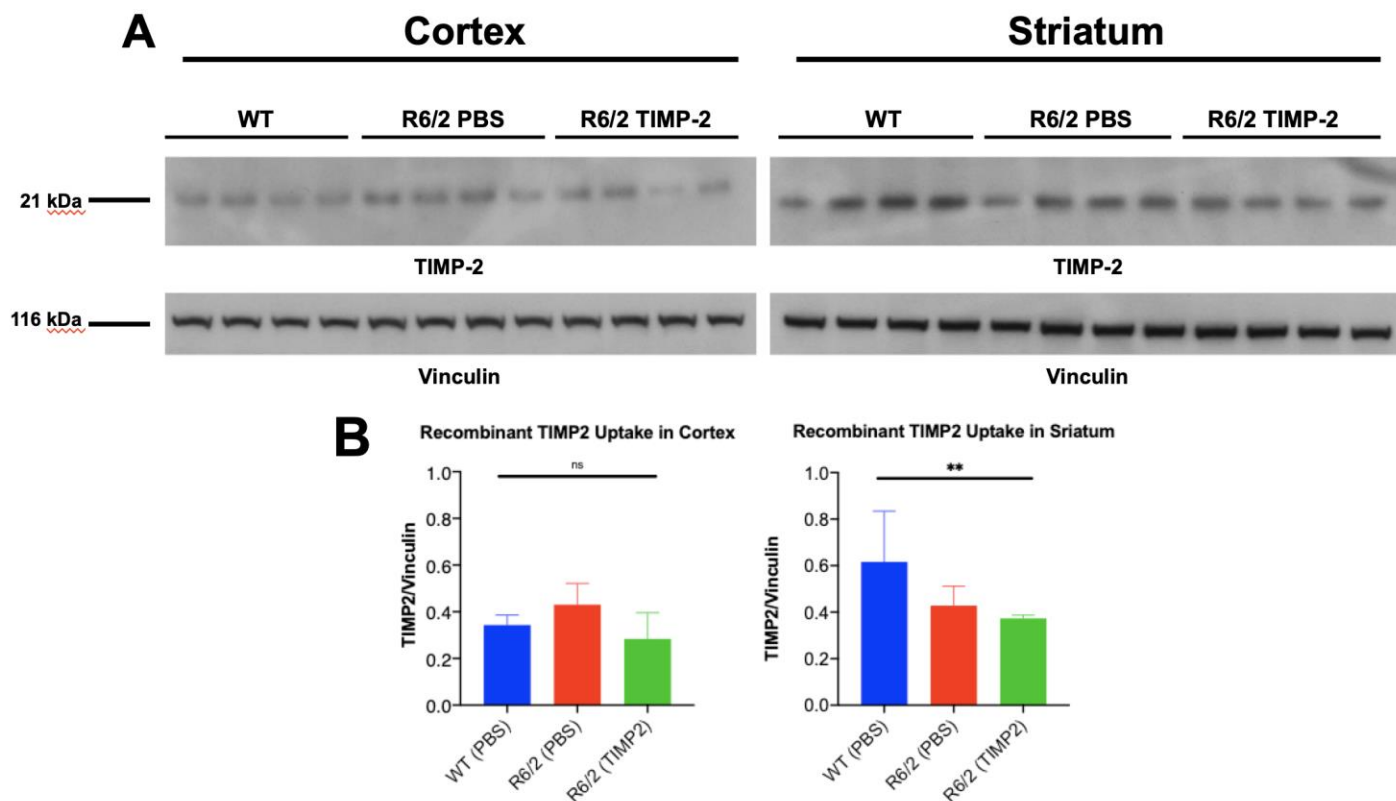


Figure 5. Western blot analysis of cortical and striatal lysates from WT mice, HD mice treated with PBS, and HD mice treated with the recombinant TIMP2. Mice were treated at 10 weeks of age and harvested at 12 weeks. After treatment with PBS or IP injection of TIMP2 protein at 0.05 $\mu\text{g}/\text{kg}$ for 17 days. A) Western blot images of the cellular lysates from these mice were probed with antibodies to TIMP2 and vinculin. B) Densitometry of the two images normalized against vinculin. Lower levels of TIMP2 were present in the TIMP2 treated mice which was not expected.

Minor Changes in Levels of Phosphorylated ERK with Systemic Introduction of TIMP2

The MEK/ERK pathways aids in cellular proliferation and is regulated by TIMP2. (Pittayapruek, Meephansan, Prapapan, Komine, & Ohtsuki, 2016). In case the levels of recombinant TIMP2 were not detectable at the protein level but still the activity was increased we tested downstream pathways modulated by TIMP2. We evaluated the MAP/ERK pathway with western blotting (Figure 6). The levels of pERK1 were not altered in the TIMP2 treated mice in the cortex again suggesting the protein did not cross the BBB. However, in the striatum

it appears the levels of pERK were normalized to WT levels. This result should be viewed cautiously as the error bars are large for both the WT and the TIMP2 treated group.

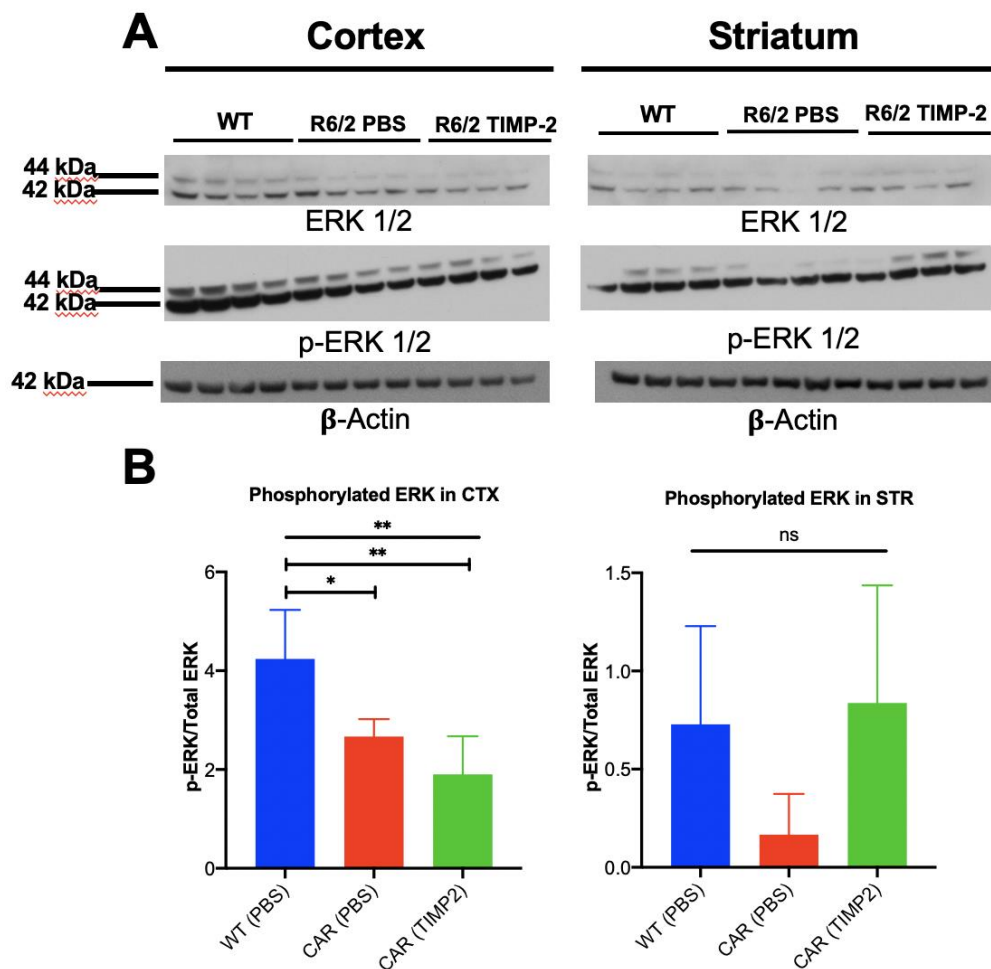


Figure 6. Western blot images of the levels of phosphorylated ERK and total ERK in the cortex and striatum of WT, PBS and TIMP2 treated R6/2 mice. Lysates processed from 3-month-old mice. A) Probing for ERK and vinculin were performed in 5% BSA to minimize background noise. B) Quantification completed with ImageQuant. Amount of p-ERK is reduced in the cortex with no rescue after TIMP2 introduction. Striatal p-ERK levels were brought back to regular levels when compared to the WT treated in PBS.

RNA-Sequencing Analysis Shows Dysregulation of TIMPs and MMPs in Medium Spiny Neurons

An important question to address is whether the TIMPs are dysregulated in human models which model medium spiny neurons, the cell type lost in HD striatum during disease

progression. We differentiated low passage corrected neural stem cell (C116) and the HD neural stem cells into MSNs and collected RNA and protein for analysis. HD medium spiny neurons have numerous alterations in MMP family members with many of the MMPs upregulated in the RNA levels as shown in Figure 7A. However, presence of TIMP2 seems to be downregulated after performing a western blot as shown in Figure 7B,C. From the densitometry analysis, protein levels of TIMP2 are much higher in the corrected cell lines of MSNs. This leads us to believe that TIMP2 may actually be upregulated during RNA transcription but it is not being produced into protein. The down regulation of TIMP2 protein in the MSNs may correlate with the increased vulnerability of this cell type in HD.

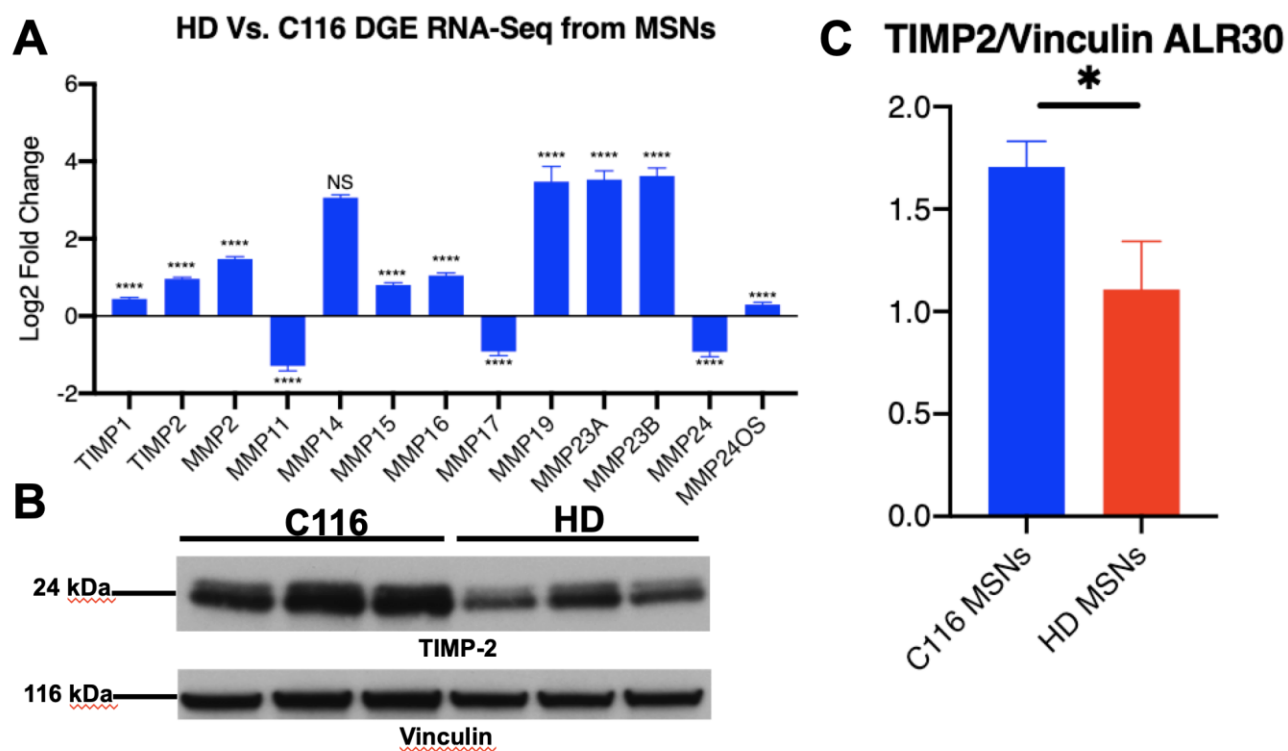


Figure 7. RNA-sequencing analysis, western blotting, and quantification of western blot from medium spiny neurons. A) RNA-sequencing showing differential gene expression levels of HD vs. C116 in medium spiny neurons. The RNA-sequencing samples and data set were generated by Dr. Kizito-Tshitoko Tshilenge. Data was mined and shown for MMP and TIMPs. B) Western blot analysis of the medium spiny neurons probed with anti-TIMP2. C) Quantified western blot using ImageQuant software. The levels of TIMP2 should be drastically raised according to the RNA-sequencing data yet do not hold true when protein quantification was performed. Possibility of RNA translation malfunctions.

Discussion

The role of MMP and TIMPs in Huntington's disease is relatively unexplored with only a few studies carefully evaluating this pathway (Li et al., 2020; Naphade et al., 2017; Rivera, 2019; Rivera et al., 2019). Previous studies in our laboratory suggested that MMPs are therapeutic targets for HD. One of the mechanisms in which these proteases may be neurotoxic is through cleavage of the mHTT protein into neurotoxic fragments. We hypothesized that the dysregulation of MMPs and TIMPs may play a significant role in HD disease progression. Therefore, our study was directed at evaluating if their tissue inhibitor, TIMP2, was altered in models of HD and if modulation of this pathway with recombinant or viral TIMP2 may provide a therapeutic for the disease.

First, we evaluated MMP activity and TIMP2 levels in two-well characterized HD mouse models, R6/2 and zQ175. These two models recapitulate aspects of the symptoms seen in affected humans. The levels of MMPs and TIMP2 in these two mouse models were altered. We found an increase in MMP2 activity in the R6/2 mouse model. Further evaluation of the TIMP2 levels in both HD R6/2 and zQ175 mice demonstrated an increase in TIMP2 in the cortex and striatum.

The analysis of HD mouse tissue by western blot will provide information on the overall expression level of proteins in all cell types in a region of the brain including neurons, endothelial cells and glia. The regulation of MMPs and TIMPs is likely to be distinct in different cell types of the brain and analysis of mouse models may not fully recapitulate the human disease. To overcome these limitations, we characterized the levels of TIMPs and MMPs in a human model of HD derived from patient-induced pluripotent stem cells. In particular, we differentiated the iPSCs into the cell type from in the striatum called medium spiny neurons.

MSNs are lost during HD disease progression and therefore are particularly interesting to evaluate MMPs and TIMPs. From our transcriptomic analysis of HD MSNs using RNAseq, we found a wide variety of MMPs were upregulated including MMP2, -15, -16, -19, -23A and -23B. TIMP1 and 2 were also upregulated in HD MSNs when compared to C116 MSNs. When we evaluated the protein levels TIMP2 in human MSNs, interestingly, we found the levels of TIMP2 were downregulated. The levels of TIMP2 may be lower due to increased degradation of the protein or perhaps altered secretion outside the cell into the media.

We established fluorometric and zymography assays to evaluate the dysregulation of MMP2 and MMP9 in our HD-patient derived cell cultures as well as in R6/2 mice. We also established the assay to measure the effect modulating the levels of TIMP2 on MMP activity. Previous studies by *Li et al.* showed that in order for the inactive pro-MMP2 to convert fully into the functional MMP2, it requires the assistance of TIMP2 and MMP14. As the amount of active MMP2 increases in the zymography, it is likely the levels of TIMP2 and MMP14 are impacted.

Systemic introduction of TIMP2 is known to repress most of the MMPs in the body. This reduction of MMP can lead to the rescue of motor deficits as well as help improve synaptic plasticity (Castellano et al., 2017). 50 µg/kg of recombinant TIMP2 was introduced to R6/2 mice for 11 days. Both biochemical and behavioral tests were performed. We evaluated their motor function using the rotarod behavioral assay and found an improvement upon treatment with TIMP2 protein. This did not correlate with our biochemical analysis as we did not detect a change in MMP2 activity or an increase in TIMP2 levels or activity with TIMP2 treatment. We will continue to optimize the delivery of TIMP2 to HD mouse models using alternative delivery strategies such as viral-mediated delivery of TIMP2 for our future studies.

Chapter 2

Abstract

Huntington's disease is an autosomal dominant neurodegenerative disease characterized by motor, cognitive, and psychiatric symptoms (Saudou & Humbert, 2016). Neuronal loss begins in the striatum and the cortex due to the expression of the mutant Huntingtin protein. The disease symptoms will begin around the age of 40 and at this time the brain has begun to atrophy. Reactive microglia and astrocytes contribute to HD and neuronal loss. Consistent with chronic inflammation numerous pro-inflammatory proteins are elevated HD plasma, CSF and post-mortem brain tissue. Despite the presence of chronic inflammation in HD, very few targeted studies have been carried out. In this study, we treated the increase of proinflammatory cytokines that would lead to gliosis with an experimental therapeutic, MW151, a selective attenuator of IL-1 β and TNF α . To attenuate neuroinflammation, we treated HD transgenic R6/2 mice starting from 6 weeks of age until death intraperitoneally at 2.5mg/kg with MW151. We found that MW151 increased the lifespan by one week in HD transgenic R6/2 mice compared to the nontreated mice. Weight loss and the deficits in heart function were slightly attenuated in the R6/2 treated mice compared to controls. Treatment with MW151 did not improve motor function as measured by grip strength, rotarod, limb clasping or open field. Further, we did not detect an improvement in learning and memory as measured by novel object assay and synaptic protein loss. The modest impact of MW151 suggests attenuation of cytokines IL-1 β and TNF α are not sufficient to improve HD disease progression.

Aim

Specific Aim 1: MW151 has been shown to reduce inflammation and reduce the enzymatic activity of MMPs. Most important, the drug efficaciously crosses the blood brain barrier (BBB) as measured using liquid chromatography-mass spectrometry. MW151 will be introduced into an HD R6/2 mouse and its efficacy will be assessed in these mice by performing behavioral studies that include rotarod, open field, novel object, metabolic cages, and hind limb clasping. Biochemical assays will also be performed including western blot, gelatin zymography, immunohistochemistry, and fluorometric assay.

Introduction

Huntington's disease is an autosomal dominant neurodegenerative disease where patients display progressive motor loss, psychiatric distress, and cognitive decline (Saudou & Humbert, 2016). The disease is a rare genetic disorder affecting 5-10 individuals per 100,000 and with typical age of onset between 40-50 years (Saudou & Humbert, 2016). HD is caused by a polyglutamine expansion encoding by a CAG repeat in exon 1 of the HTT protein. One of the hallmarks of HD patient postmortem tissue is the massive gliosis with reactive microglia populating the striatum and cortex suggesting that neuroinflammation is a key part of disease pathogenesis. In addition, *in vivo* positron emission tomography (PET) scans of patients with HD, using biomarkers for activated microglia (C-PK11195) and markers for dopamine D2 receptor binding sites (C-raclopride) which track striatal GABAergic cell function (Rocha et al., 2016) show a significant binding of C-PK11195 along with a reduction of C-raclopride binding in the striatum and cortex (Rocha et al., 2016). Over time, patients that came back for more imaging, showed increasing numbers of C-PK11195 binding and an even lower amount of C-raclopride binding. While there are some options to mitigate HD symptoms, there are no known cures for the disease. Our study will focus on the gliosis of HD and reducing proinflammatory cytokines with a highly selective suppressor, MW151.

Neuroinflammation in the HD brain does not comprise of the infiltration of peripheral immune cells into the brain due to a pathogen. Instead, inflammation is brought on by the resident glial cells in the brain known as astrocytes and microglia. Under stress by radiation, traumatic brain injury, or neurodegenerative disease the glial cells become activated. mHTT is expressed in all cell types of the brain. In HD, inflammation is due in part to the expression

of mHTT in the to the glial cells. In microglia, the genetic modification causes an increase of expression and transcriptional function of myeloid progenitors, PU.1 and C/EBP (Crotti & Glass, 2015). HD patients have enriched areas of binding sites and promoters in PU.1 and C/EBP transcription factors which were detected by ChIP-Seq. In astrocytes, there is an abnormal increase of the nuclear factor kappa B (NF- κ B) pathway which is responsible for the regulation of pro-inflammatory mediators when stimulated (Rocha et al., 2016).

Upstream of the NF- κ B pathway is an enzyme complex called I kappa B kinase (IKK) in which can keep the NF- κ B pathway activated for longer periods of time creating another feed forward loop (Rocha et al., 2016). In addition to the increase in transcription, mHTT affected astrocytes do not allow for the uptake of glutamate and prevent the secretion of chemokine ligand 5 (CCL5). This is particularly detrimental for medium spiny neurons because they required glutamate for regular synaptic function (Crotti & Glass, 2015).

MW01-2-151 [2-(4-(4-methyl-6-phenylpyridazin-3-yl) piperazin-1-yl) pyrimidine] (MW151) is a novel therapeutic that has been previously used to treat Alzheimer's Disease mice, traumatic brain injury (TBI) models, and closed head injury (CHI) models (Bachstetter et al., 2012; Bachstetter et al., 2016; Webster, Van Eldik, Watterson, & Bachstetter, 2015). This therapeutic drug is water soluble, chemically stable, central nervous system (CNS)-penetrant, and with a brain: blood ration >1 , making this similar or better than current CNS drugs currently being used (Hu et al., 2007). MW151 is also metabolically stable, maintaining $>90\%$ of the drug in the body even after 2 hours from administration. This therapeutic, in general, is safe with minimal to no histological liver toxicity regardless of high or low dosages and presents no evidence of cardiovascular toxicity (Hu et al., 2007). In a previous study performed by *Bachstetter et al.*, treatment with MW151 conferred

neuroprotection against synaptic protein loss and improvement of synaptic plasticity (Bachstetter et al., 2012). The same group also noticed significant rescue in cognitive behavior in an AD, CHI, and TBI mouse model if treated within the window of treatment (Bachstetter et al., 2012; Bachstetter et al., 2016; Webster et al., 2015). These results show positive and concrete outcomes for mice in both neurodegenerative disease models and traumatic brain injury models. Further, an improved version of the molecule, MW189, has passed Phase I safety, tolerability, pharmacokinetic and pharmacodynamic studies in humans for use in acute brain injury (Van Eldik et al., 2020). We therefore decided to evaluate MW151 in a preclinical study with the Huntington's disease mouse model, R6/2.

MW151 targets proinflammatory TNF- α and cytokine IL-1 β (Van Eldik et al., 2020). TNF- α levels are increased in the brains and plasma of HD patients and mouse models and modulation of this pathway has been evaluated using etanercept in HD mice (Pido-Lopez et al., 2019). Here, we investigated whether MW151 has beneficial consequences in suppressing neuroinflammation. We treated transgenic HD R6/2 mice with MW151 which led to a modest decrease of pro-inflammatory markers. We measured rotarod, open field, clasping, grip strength, weight, lifespan, novel object test and metabolism with metabolic cages during treatment with MW151. Further characterization of the R6/2 mice heart was conducted using echocardiographs. As discussed below, we believe the novel compound could lead to a successful therapeutic treatment for some aspects of Huntington's disease. However, this will require further studies at a different dose and more analysis of the full effects of the compound.

Methods

Synthesis and Use of MW151

MW01-2-141SRM (2-(4-(4-methyl-6-phenylpyridazin-3-yl)piperazin-1-yl)pyrimidine was synthesized and characterized as previously reported (Hu et al., 2007). MW151 is a water soluble, chemically stable, small molecule (molecular weight: 423). It is non-toxic to liver and cardiac function. MW151 is CNS-penetrant with a blood-brain ratio of >1. Compound MW151 is not a pan-suppressor of neuroinflammation and specifically inhibits IL-1 β and TNF α , but not IL-10 (Bachstetter et al., 2016; Hu et al., 2007; Webster et al., 2015). 318.7 mg of powdered compound was added to 33.37 mL of saline solution (0.9% sterile saline, Hospira NDC0409-4888-10). Stock concentration was 9.55 mg/mL and diluted 1:10 in saline for working concentration of 0.955 mg/mL solution. MW151 compound was administered by intraperitoneal injection at a working concentration of 2.5 mg/kg. Saline was injected intraperitoneally as the vehicle control.

R6/2 Mouse Brain Dissections

Mice were anesthetized with isoflurane and the cervically dislocated. An adult mouse brain matrix (Bioanalytical Systems, RBM-2000c) with 1 mm coronal slices was used to slice the brain further. Hippocampal, cortical, striatal, cerebellum, and brain stem were dissected. All sections were dissected over ice and immediately flash frozen over dry ice. Organs such as heart, kidney and kidney were also collected. Samples were stored at -80°C until needed.

Bicinchoninic Acid Assays and Western Blots of Mouse Brains

R6/2 and control mice treated with MW151 and vehicle control were euthanized and brain regions and organs collected at 12 weeks of age. Samples were lysed with a combination of 10 mL of tissue protein extraction reagent (TPER) and one tablet of Roche complete protease inhibitors. They were then processed further via sonification under protocol of 5 seconds of pulsing and 5 seconds of rest for 5 rounds at 40 mA. Samples were then spun down at 14,000 rpms at 4°C for 20 minutes and quantified under a BCA assay. Amounts of protein between 10-20 µg were added to 1µL of DTT and LDS Nu-Page buffer. Proteins were boiled at 95°C for 10 minutes. SDS-PAGE gels were used in this western blot and they were run at 200 V for 1 hour. Gels were then transferred over to a polyvinylidene difluoride membrane overnight at 20V in a 4°C cold room. Membranes were then blocked with 5% non-fat milk for 1 hour. Primary antibodies were added to the membrane and probed overnight at 4°C. Washes (3X) with 1X TBST were performed for the removal of excess primary antibody and then the secondary antibody was added and kept on for 1 hour at room temperature. Membranes were then washed (3X) once again in 1X TBST and imaged with Pierce enhanced chemiluminescence reagents (Thermo Scientific).

Rotarod

Motor performance was assessed using rotarod analysis. Rotarod was performed on mice post drug treatment for a period of 3 consecutive days during their day cycle at weeks 7, 9, 11, 13, 15, and 17. Each day consisted of an acclimation session which kept mice on the rotarod at a constant 5 rpm for 5 minutes followed by a 3-trial run where the wheel would accelerate (5 – 50 rpm) for a total of 6 minutes. Any mice that fell off the rotarod during the acclimation period

were placed back on the machine until the completion of their 5 minutes. Mice that fell off during the trial period were placed back into their respective cages.

Open Field

Open field assessment was performed during the mice's dark cycle at weeks 5, 9, 12, and 14. Prior to testing, mice were held in a dark room in complete silence for 30 minutes in order to acclimate them to their surroundings. Mice were then placed in a field box and their horizontal and vertical movements were recorded for 10 minutes. Mice were then returned to their cages.

Elevated Plus Maze

This elevated plus maze was performed during the mice's light cycle and were tested at week 11 and 13. No acclimation period was needed other than lowering the amount of light in the room. Mice were placed on the elevated plus maze and were allowed to move freely between two open arms or two enclosed arms for 10 minutes. Any mice that fell from the maze were checked for seizure activity and placed back on the maze if no symptoms showed. Their movements were videotaped and analyzed by Noldus software.

Hindlimb Clasp

Prior to testing, mice were acclimated in a low-lit room with minimal noise for 15 minutes. Each mouse underwent a 3-trial run, each trial lasting 10 seconds. The mouse was removed from its cage, set on the table, and then lifted up by its tail at a height of 5 inches. After its 10 second trial the mouse would be scored as 0, 1, 2, or 3 according to the position of its hind legs. A score of 0 indicated its hindlegs were spread out, a 1 would have its legs slightly

clenched to its body, a 2 would have its legs closer to its body where the body would often feel stiff, and a 3 would indicate the total retraction of its limbs and curling up into a ball. Its final score was the average of the 3-trial run.

Grip Strength

Mice were not acclimated for this run and this assay was only performed at week 5 and 13. The mouse was lifted by its tail to the height of the bar where the mouse will grasp. The mouse was checked for a good grip and the investigator gently pulled on the mouse until the grip was broken. This was repeated 5 times in order for the software to average out the grip strength. Averages were recorded according to body weight, grip force, and max strength.

Metabolic Cages

Mice were single housed for 3 days in order to acclimate to the metabolic cages. After acclimation was complete, the mice were placed in a cage that contained a running wheel, sleeping house, water, and food. Food, water, and oxygen consumption was recorded by the metabolic cage every 5 minutes. Mice were left in the cage for a total of 4 days with no interruptions from other behavioral tests, injections, and cage cleaning.

Echocardiographs

Echocardiography was carried out by a skilled operator using a Visualsonic 3100. Metrics of cardiac function were calculated from 3 different views, parasternal long-axis view, short-axis view, and apical 4-chamber view. Typical metrics of function included (but were not limited to) systolic and diastolic measures such as ejection fraction(systolic), fractional shortening (systolic), strain (systolic

and diastolic), and mitral valve function (E/A - diastolic). Calculations for such metrics were derived via a custom script written in R.

Results

Study design for behavioral tests in R6/2 mice with MW151

In order to evaluate MW151 in R6/2, we developed the study plan shown in Figure 1. Prior to treatment mice were randomized into their treatment groups according to their body weight and baseline performance on rotarod and grip strength at 5 weeks of age. The study was carried out blinded with the solutions provided to us as A and B. At 6 weeks of age, daily IP injection of WT and R6/2 was initiated at a dose of 2.5 mg/kg or vehicle for behavioral studies with an N= 15 per group for the R6/2 mice and N = 10 for the WT mice. Additionally, WT and R6/2 were injected at a dose of 2.5 mg/kg and vehicle from 6 weeks of age until 12 weeks for histology and western blot analysis (N=7-8 per group).

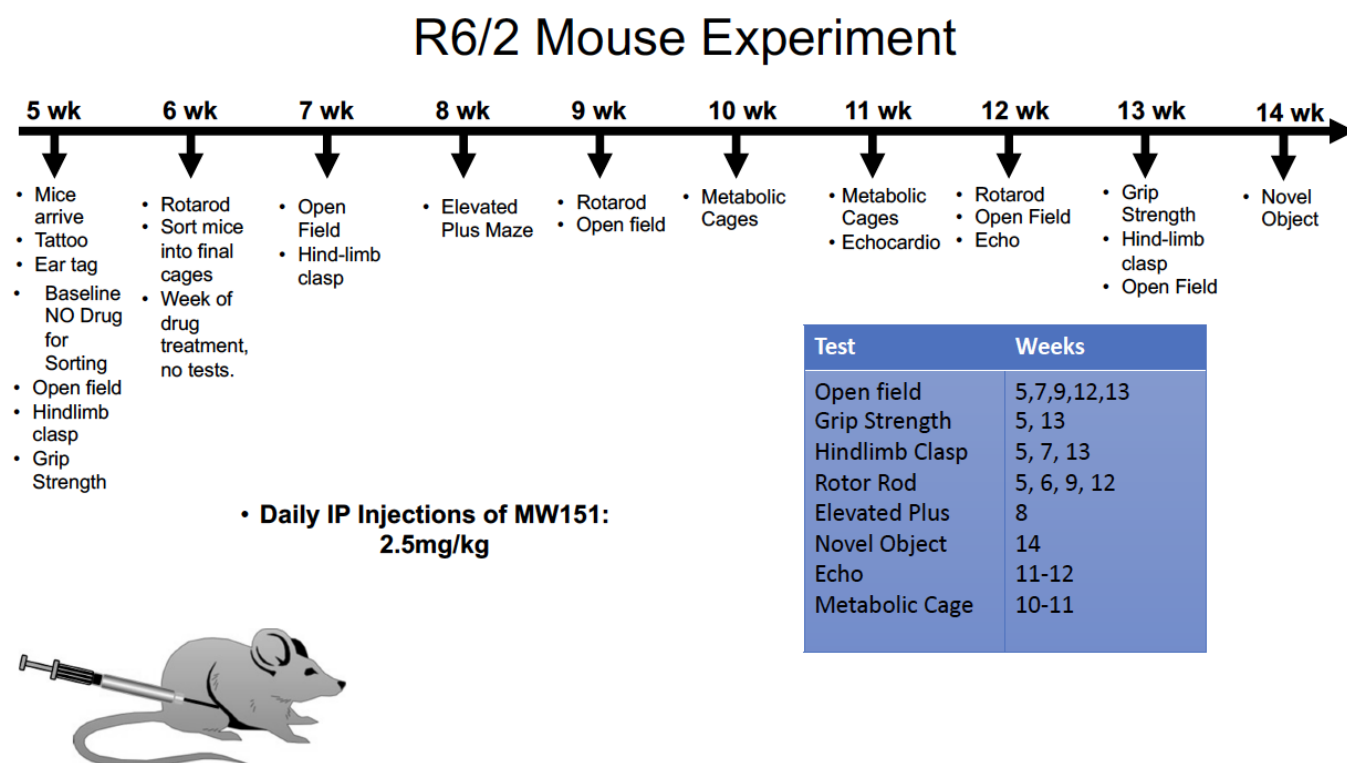


Figure 1. Study design for behavioral tests in R6/2 mice with MW151. All mice were kept under minimal lighting and at low volumes of noise. Compound MW151 will be used in both WT and HD models for full evaluation.

MW151 treatment reduces weight loss in both WT and R6/2 carrier mice

Huntington's disease patients are known to lose large amounts of weight as the disease progresses. This is due to altered energy metabolism, increased movement and other psychological issues affecting food intake. Starting at 5 weeks of age, we measured the weight of WT and R6/2 mice with and without MW151 treatment as shown in Figure 2. Consistent with previous data, the R6/2 mice failed to gain weight when compared to WT mice. During the disease progression the R6/2 mice lost weight and treatment with MW151 attenuated weight loss. This was statistically significant at day 147. Further, the MW151 treated mice in both genotypes consistently maintained their weights above the untreated mice. This positive trend may indicate that the compound affects symptoms relevant to metabolism, motivation or food intake.

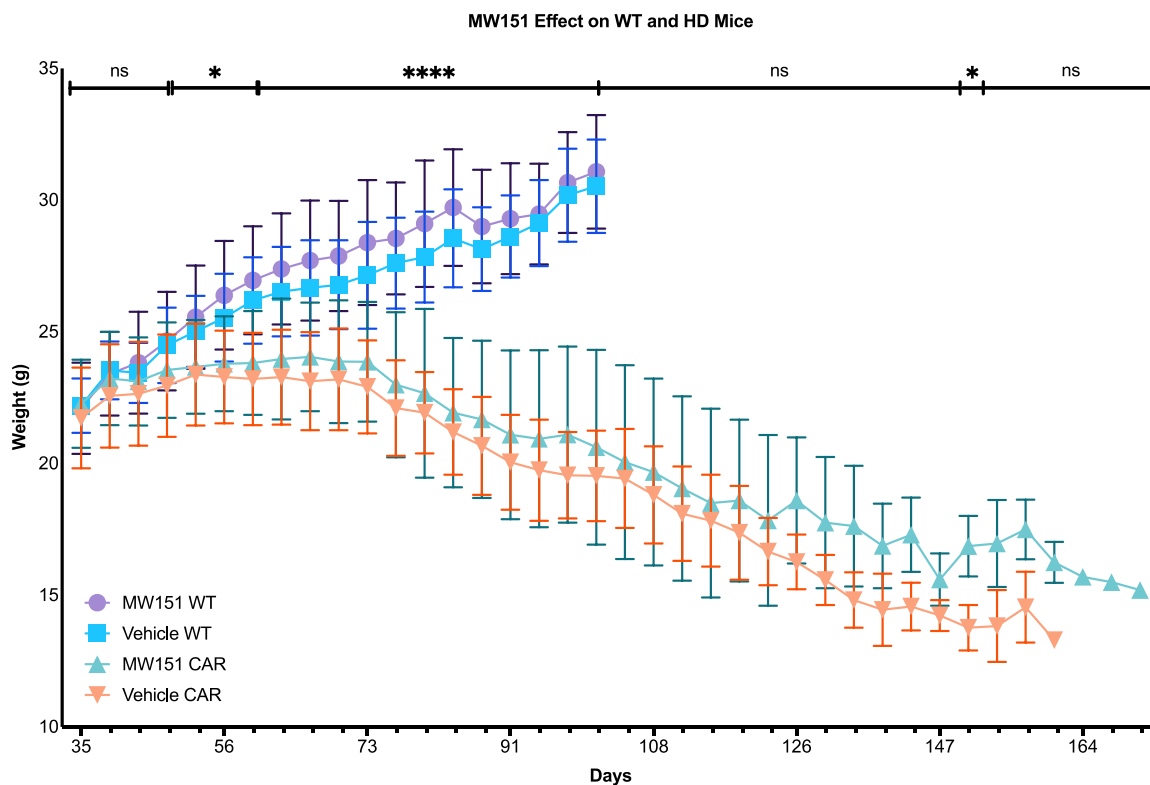


Figure 2. The weight of mice was recorded every Tuesday and Friday. Statistics shown from day 35 to day 101 are comparisons between WT and carrier mice (HD R6/2 mice). After day 101, the comparisons

are between treated and untreated carrier mice only. One-way ANOVA and student t-tests performed on this data.

Rotarod results show no improvement in mice treated with compound MW151

One of the symptoms in Huntington's disease is motor dysfunction. Patients are known to have chorea, repetitive involuntary movement. Using the accelerating rotarod assay, we can determine how much the disease has impacted the mice ability to move for an extended period of time. Mice were tested at 5, 6, 9 and 12 weeks of age.

As shown in Figure 3, R6/2 mice have impaired motor function when compared to WT mice. Treatment of the R6/2 with MW151 did not alleviate symptoms. Of note, treatment of the MW151 did not change the motor function of WT or R6/2 mice indicating compound does not negatively impact motor function.

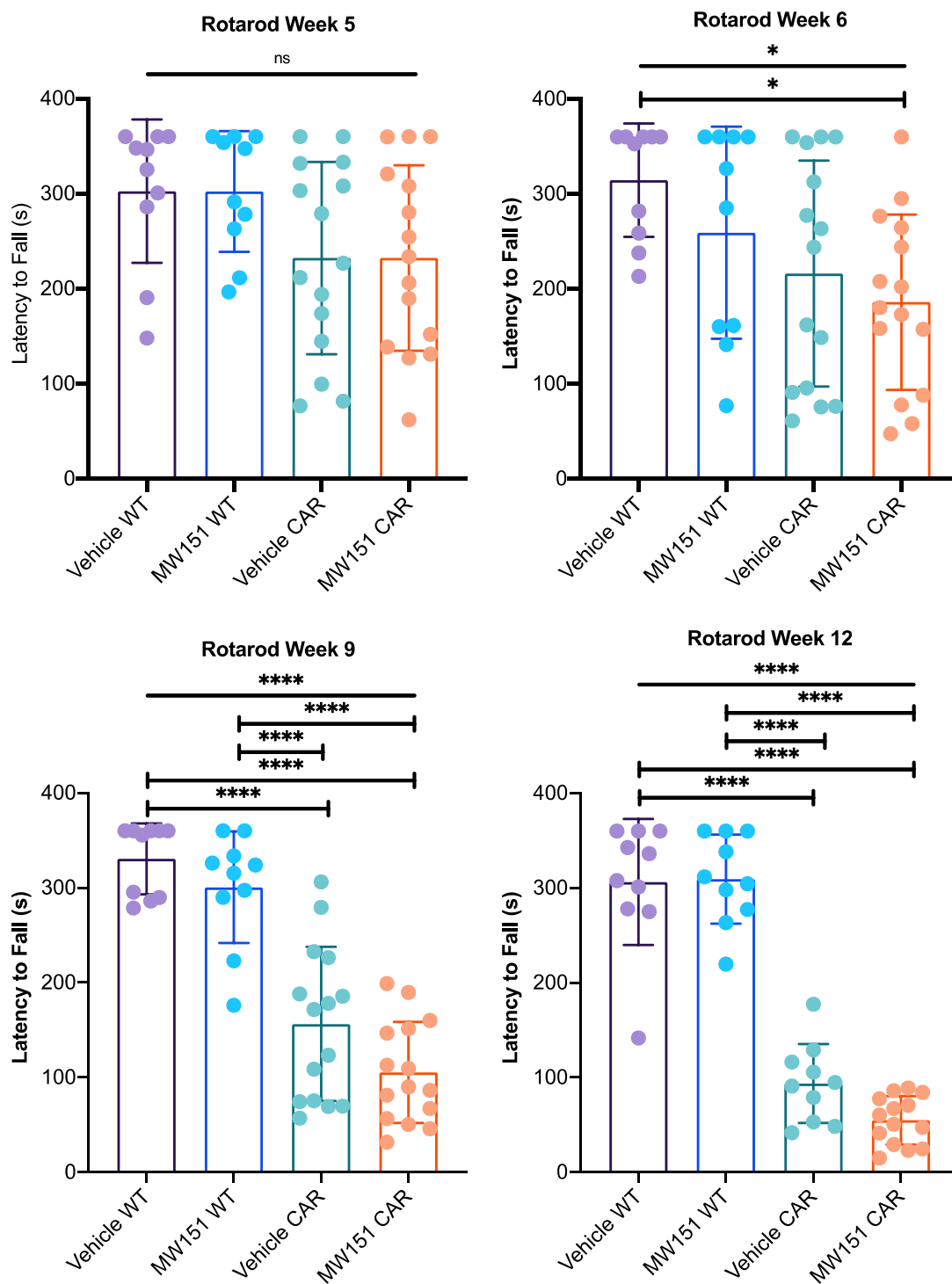


Figure 3. Rotarod analysis was performed on weeks 5, 6, 9, and 12. Treatment does not appear to mitigate the symptoms and it also does not seem to affect the mice negatively considering the WT mice treated with the compound did not lose motor function throughout their lifespan. The top most unbracketed line of significance represents comparisons as a whole performed by one-way ANOVA. Bracketed lines of significance represent student t-tests.

Anxiety levels and judgement of MW151 treated mice were unaltered

Wild type mice spend more time in an enclosed area as that is their normal behavior. In the Huntington's disease mouse model, their judgement is impaired and this can be measured by the time spent exploring open areas. We hypothesized that MW151 would attenuate inflammation and therefore relieve stress in the brain which impairs judgement.

In order to understand this phenomenon, we placed our mice in an elevated plus maze. The elevated plus maze is a test measuring the anxiety of mice. During the trial the mice are placed on a cross shaped platform consisting of two open and two closed arms placed 50-70 cm above the ground. The conflict between the innate curiosity to explore novel environment and the fear of the open arms allows evaluation of anxiety. Mice were observed for 10 minutes and then placed back in their cages. As shown in Figure 4, poor judgement in the carrier mice is exhibited by their overt explorative behavior. The R6/2 mice spend more time in the open arms of the maze and often fall off the maze when compared to WT mice (Figure 4). Treatment of R6/2 mice with MW151 did not have any effect on the mice behavior regardless of genotype (Figure 4).

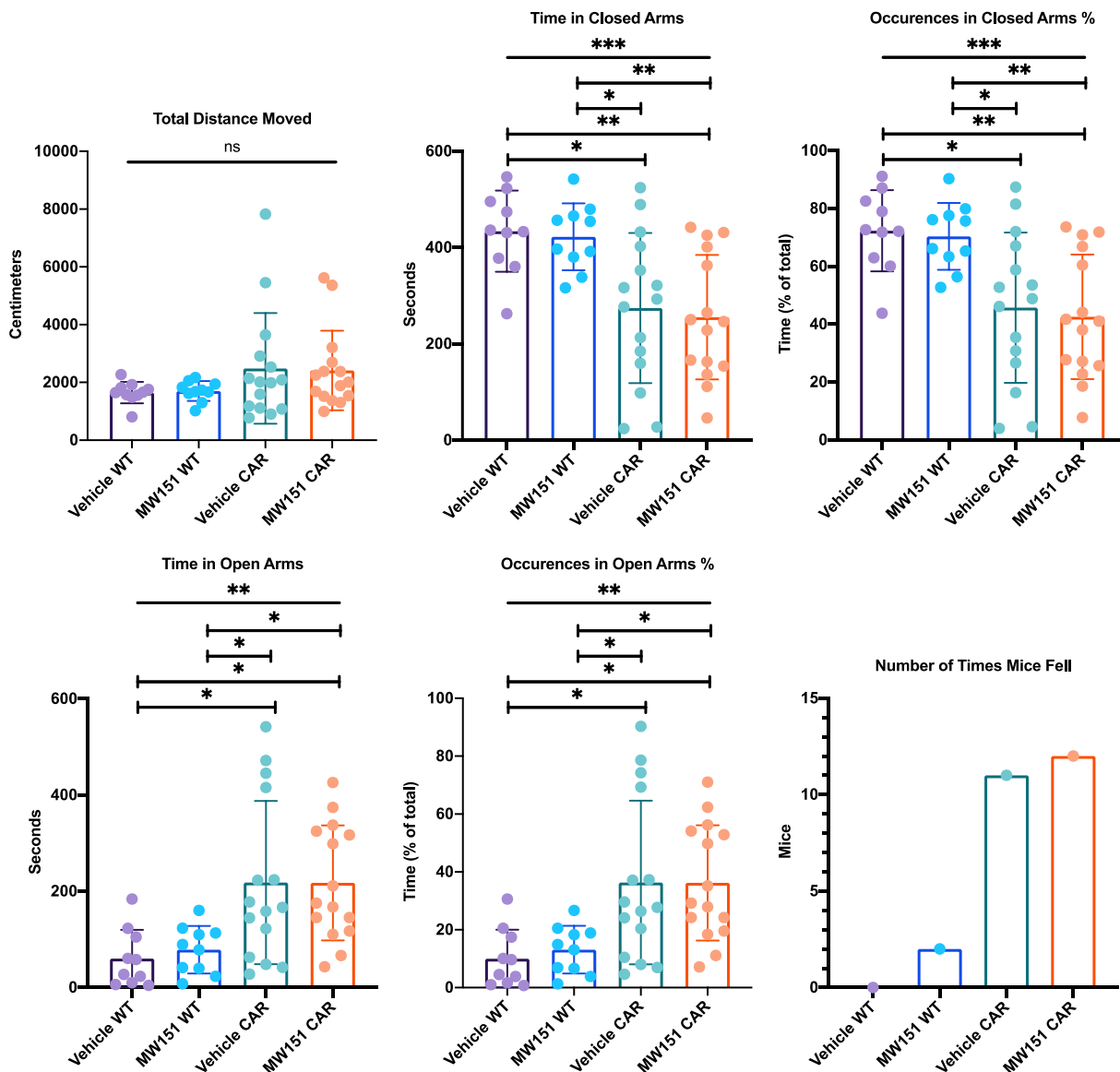


Figure 4. Elevated plus maze results. WT mice would present typical phenotypes in which they maintain themselves in closed quarters. As opposed to the R6/2 mice which are often found exploring the opened arms more than the close arms.

Grip strength assay presents no rescue of muscle atrophy in the R6/2 mouse model

Common symptoms in Huntington's disease also include muscle atrophy, the loss of muscle in the body. It's believed that muscle wasting occurs because of mHTT expression in the skeletal muscle cells where the altered disease protein impacts normal muscle function.

To measure muscle loss over time, we tested mice using a grip strength assay. The grip strength test is used to measure neuromuscular function as maximal muscle strength of forelimbs and hind limbs. Mice are placed on a small square with bars. As you pull on the mice tail, the mice hold on to the bar and at some point, will let go. This pull is their maximum force and it can be normalized to their weight ultimately calculating the total force they exerted. As shown in Figure 5, the MW151 compound did not prevent muscle atrophy at 13 weeks of age.

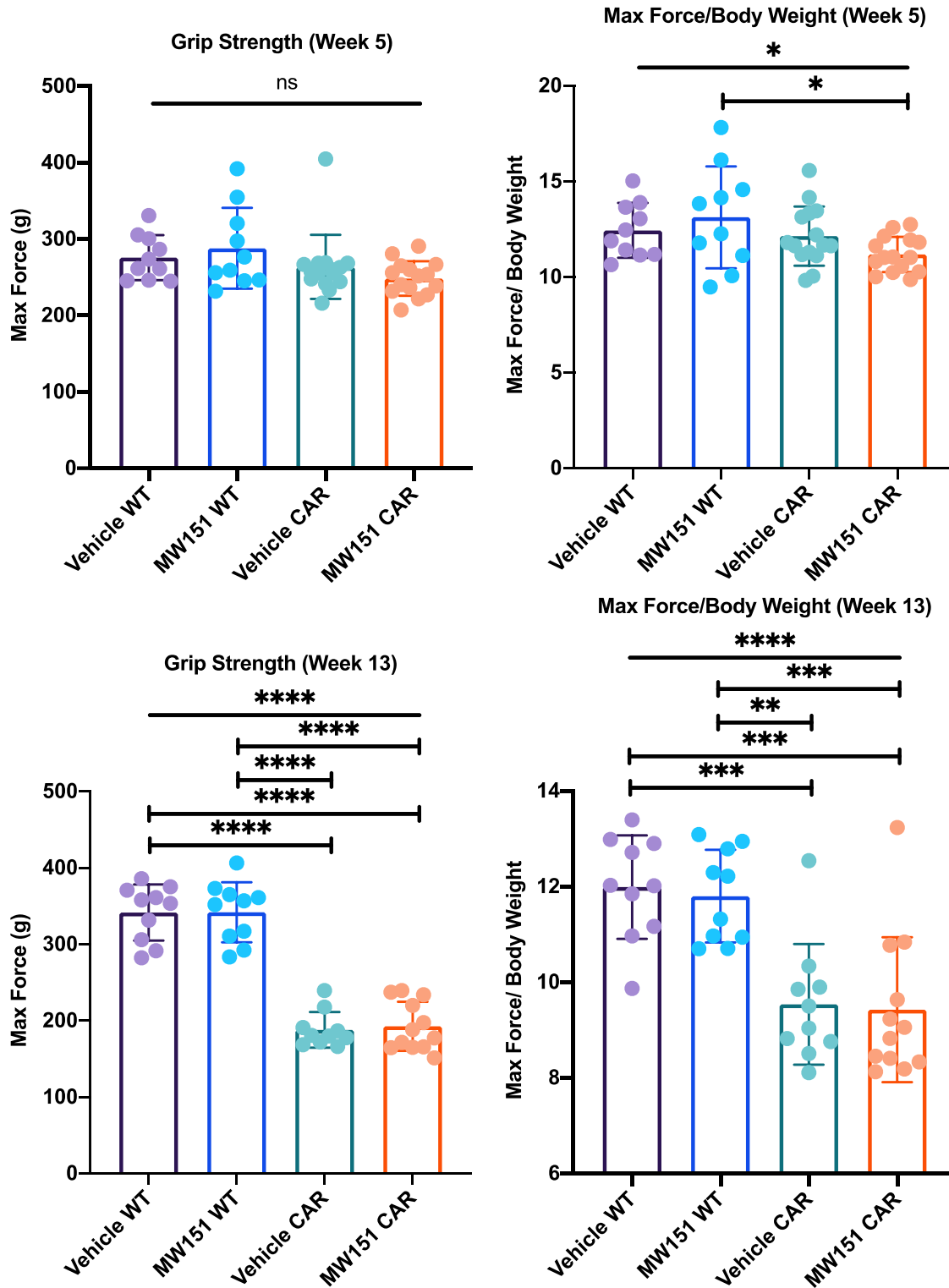


Figure 5. Grip strength assay was performed twice, once for basal levels and the second round to determine grip force. Overall, the mice displayed normal muscle loss due to age and/or genotype. No detrimental side effects on muscle and strength were present.

Hindlimb Clasping Was Not Impacted by the Treatment

Atypical behavior in Huntington's disease mice is clasping of their hindlimbs. This phenotype is observed in a variety of neurodegenerative diseases including spinocerebellar ataxia and spinobulbar muscular atrophy. The hindlimb clasp assay is a good indicator of how rapidly the disease is progressing.

As shown in Figure 6, disease progression in the R6/2 carrier mice worsens with time with an increase in hindlimb clasp. There is a positive trend in which the carrier mice treated with MW151 were not clasping as much as the saline treated carrier mice.

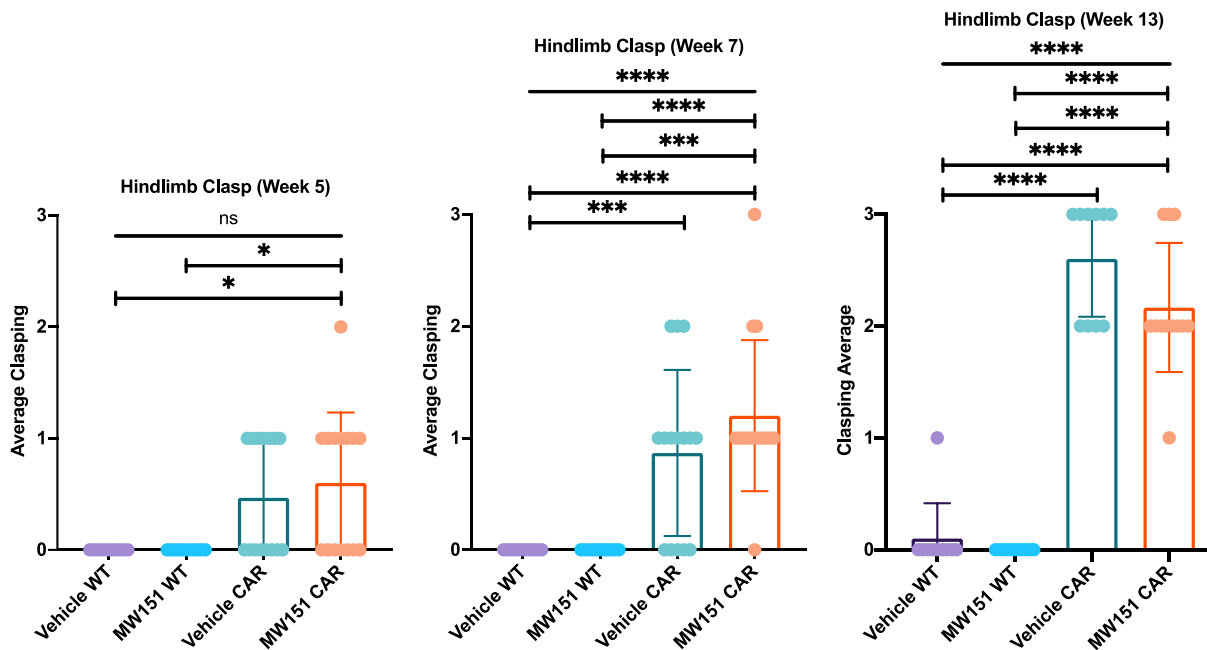


Figure 6. Grip strength assay was performed only three times in the mice lifespan. Week 5 assay was performed to receive basal levels. Only two weeks after we can see that the disease progresses rapidly making more mice clasp. At 13 weeks we have peak neurodegeneration and the carrier mice show severe symptoms and most mice averaging 2.5 to 3 scores in clasping.

MW151 treatment results in minor improvements on exploratory behavior and mobility

As previously mentioned, Huntington's disease affects motor function and influences personality both in human patients and in mice. Exploratory activity in open field was measured at 7, 9, 11 and 13 weeks of age. We performed an open field assay on the mice during their active cycle which is during the night. Open field assays allow us to observe how mice move freely in the horizontal plane and if they display interest in reaching above in the vertical plane.

As shown in Figure 7, R6/2 mice display a decrease in floor plane movement over time and other changes previously described for the HD mice when compared to WT. Although wild type mice performed normally, the MW151 treated mice showed an affinity for the vertical plane more than the saline treated mice. The same can be seen in the R6/2 carrier mice but that tendency diminishes past week 9 as the disease progresses.

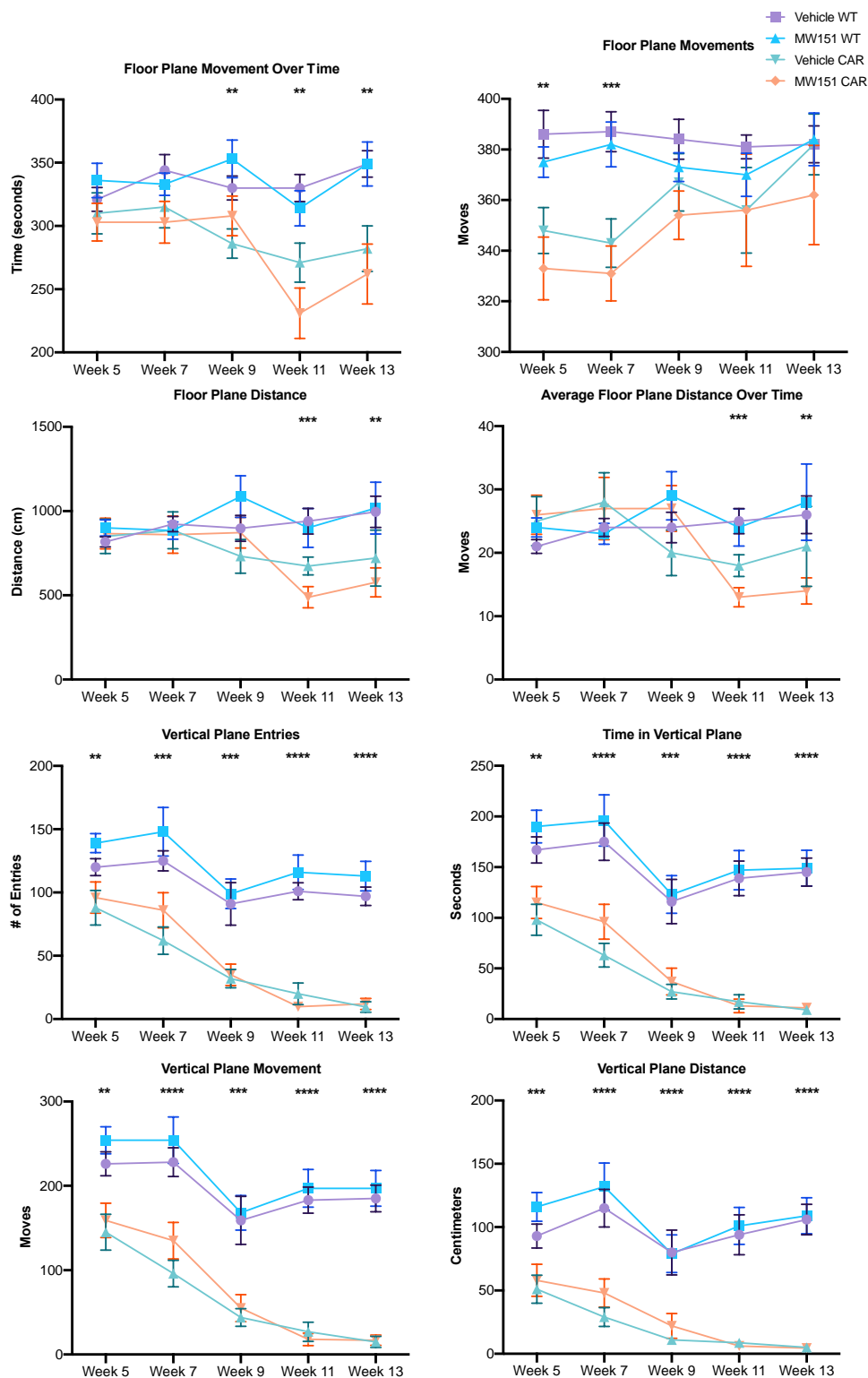


Figure 7. Open field assay presenting movement in the horizontal and vertical plane. Horizontal plane movement does not present any rescue in motor function nor behavior. Vertical plane movement shows minor improvement in MW151 treated mice. Treatment seems to be less effective as the disease progresses and the mice age. This could indicate two instances where it is not just the disease but the aging process as well.

Huntington's disease mice treated with MW151 show memory improvement

Huntington's disease is well known to cause memory loss and difficulties in learning. One of the ways we observed this hallmark of HD is through the novel object assay. In this assay, the mice would spend 10 minutes in the field "training" their mind to the two objects present in the area. These mice would then be removed and placed back into their cages and then brought back out 24 hours later and shown one novel object and one recurring object from their first test. This large time frame between tests will allow us to determine how much the mice ability to learn has declined.

The wild type mice had better discrimination of the novel object than the R6/2 mice. Although not statistically significant, it appears the R6/2 mice treated with MW151 had increased nose touch frequencies similar to the WT mice. The counts seen below in Figure 8 are performed manually by a person as well as automatically from the software that videotaped the test.

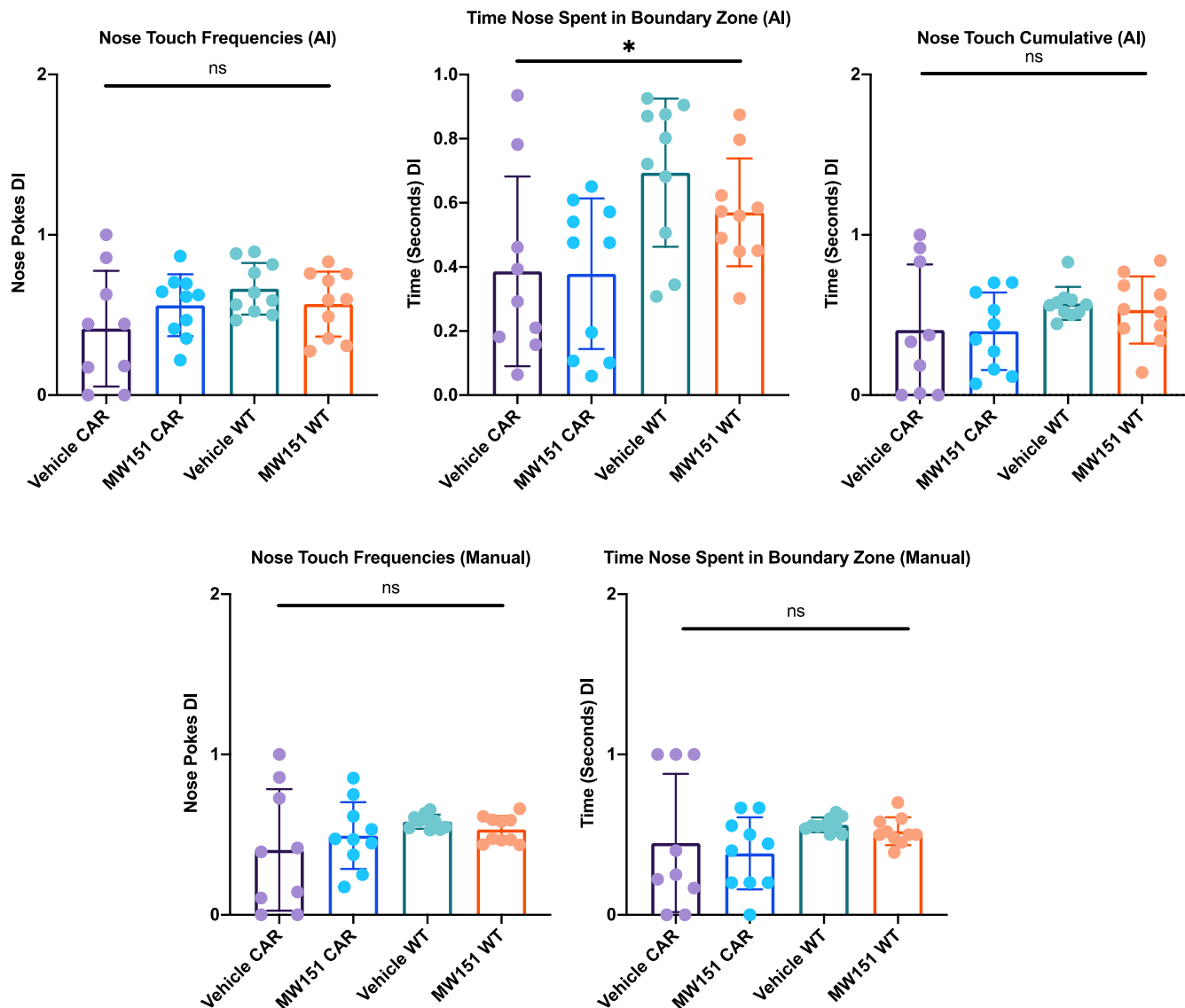


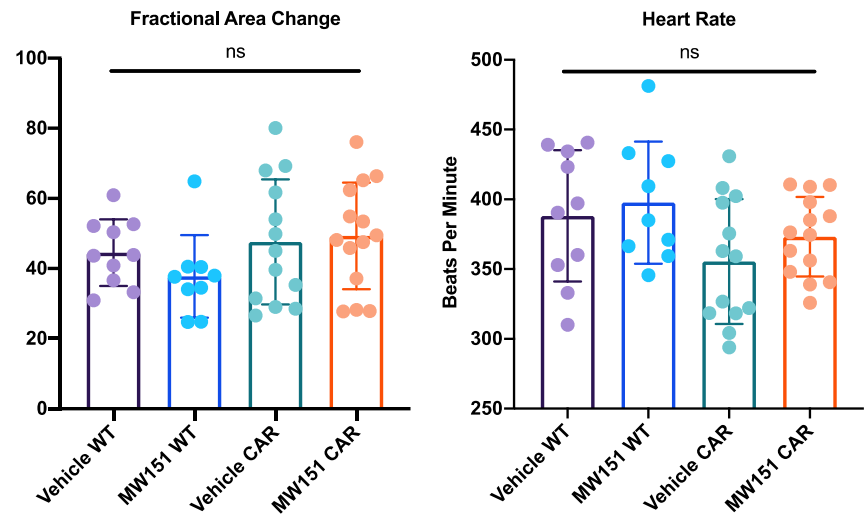
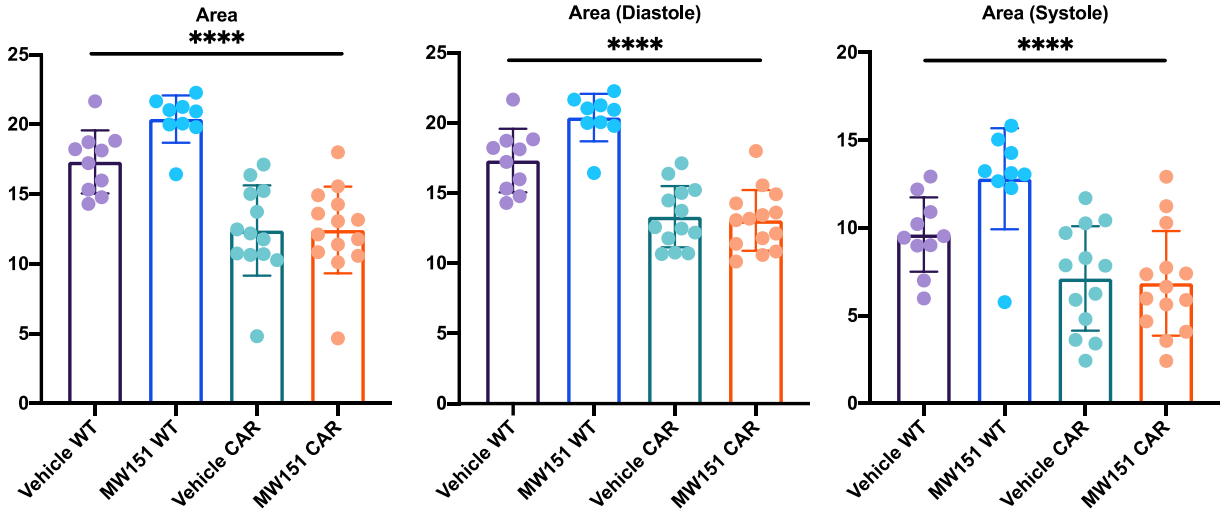
Figure 8. Novel object recognition assay performed on the mice at 13 weeks of age. A) The number of times the boundary was broken and alerted the software. B) Amount of time spent within the boundary and counted by the software. C) Number of times the software counted the mouse's nose touching the novel object. D) The number of times the boundary was broken by the mouse and counted for manually. E) Amount of times the mouse tapped the novel object and was accounted for manually.

Evaluating R6/2 cardio pathology and the effects of MW151

Heart disease is the second leading cause of death in Huntington's disease patients. The first cause of death is aspirating pneumonia. Mice with the disease are known to have reduced heart mass and arrhythmias (Mihm et al., 2007). Considering that the altered *mHTT* gene is

ubiquitous in the body, it is important to study how the mHTT protein affects organs outside of the central nervous system. The heart is the least characterized organ in this mouse model and using a selective anti-inflammatory compound may help us understand if the heart is negatively affected by innate immune responses.

HD mice treated with MW151 showed an improved heart rate when compared to vehicle treated mice. A positive trend can also be seen in their ability to pump out at least 60% of their blood out of the left ventricle and into the body as shown in Figure 9 under ejection fraction. While this may seem to improve the heart, the HD mice in both treatments still maintain smaller ventricular masses showing that their hearts are weakening as the disease progresses. The WT mice treated with MW151 show an improvement of their left ventricle and their heart rate, as shown in Figure 9.



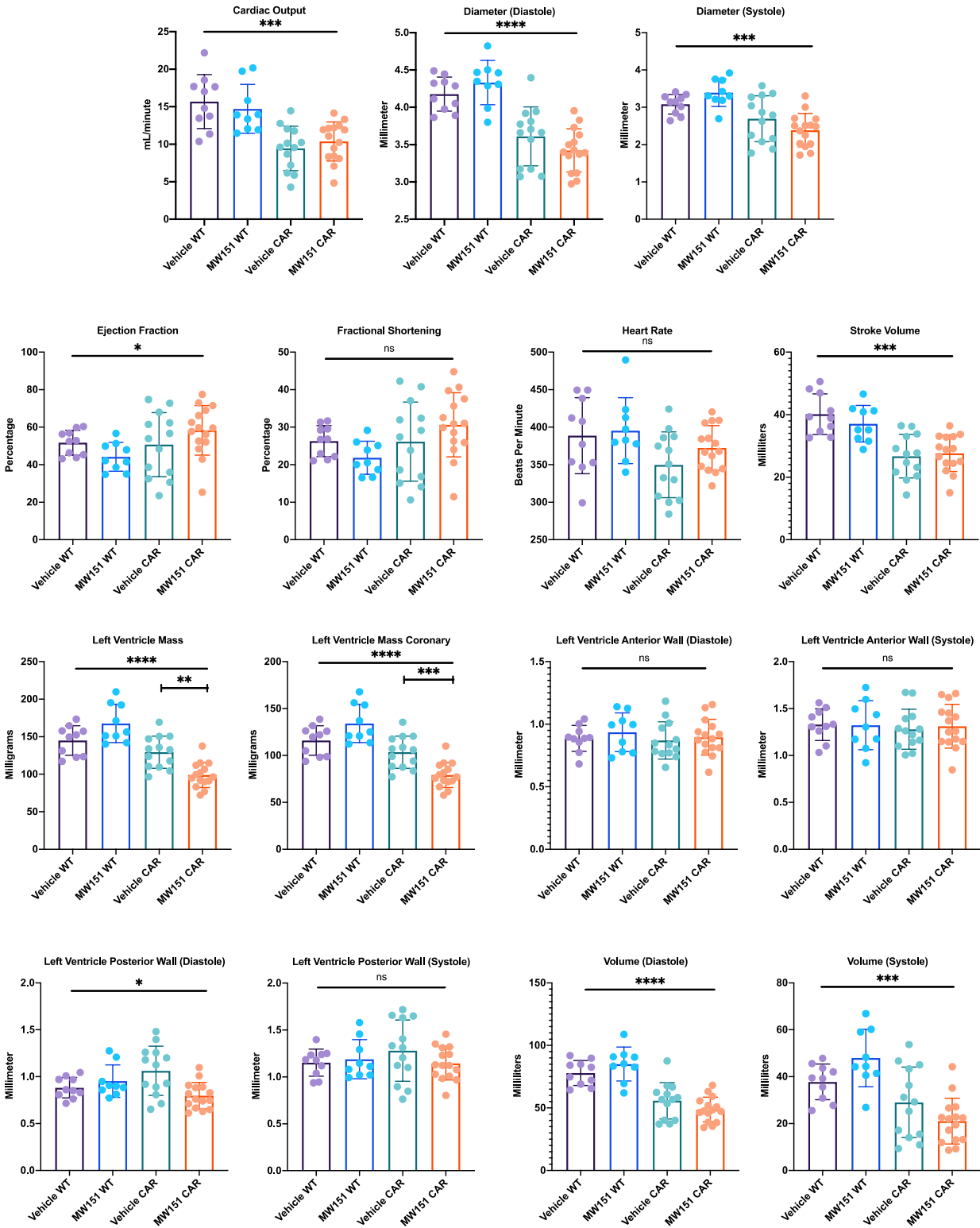


Figure 9. Short axis echocardiographs performed on 11-week-old mice. All analysis performed under one-way ANOVA and student t-tests. Images acquired using VeVo lab software from Visual Sonics.

Lifespan of MW151 HD treated mice increased

Average life span of a Huntington's disease mouse is between 13-16 weeks or 91-112 days. Some mice may last longer depending on their CAG expansion. The carrier mice treated with the compound showed positive trends with a mean lifespan of 175 days. Meanwhile, the saline treated carrier mice had a mean lifespan of 163 days (Figure 10). It is possible with an increase in dosage of the compound, the lifespan in these mice could drastically improve. In addition to their lifespan we would also rescue the loss of synaptic proteins, neurons, and ultimately memory.

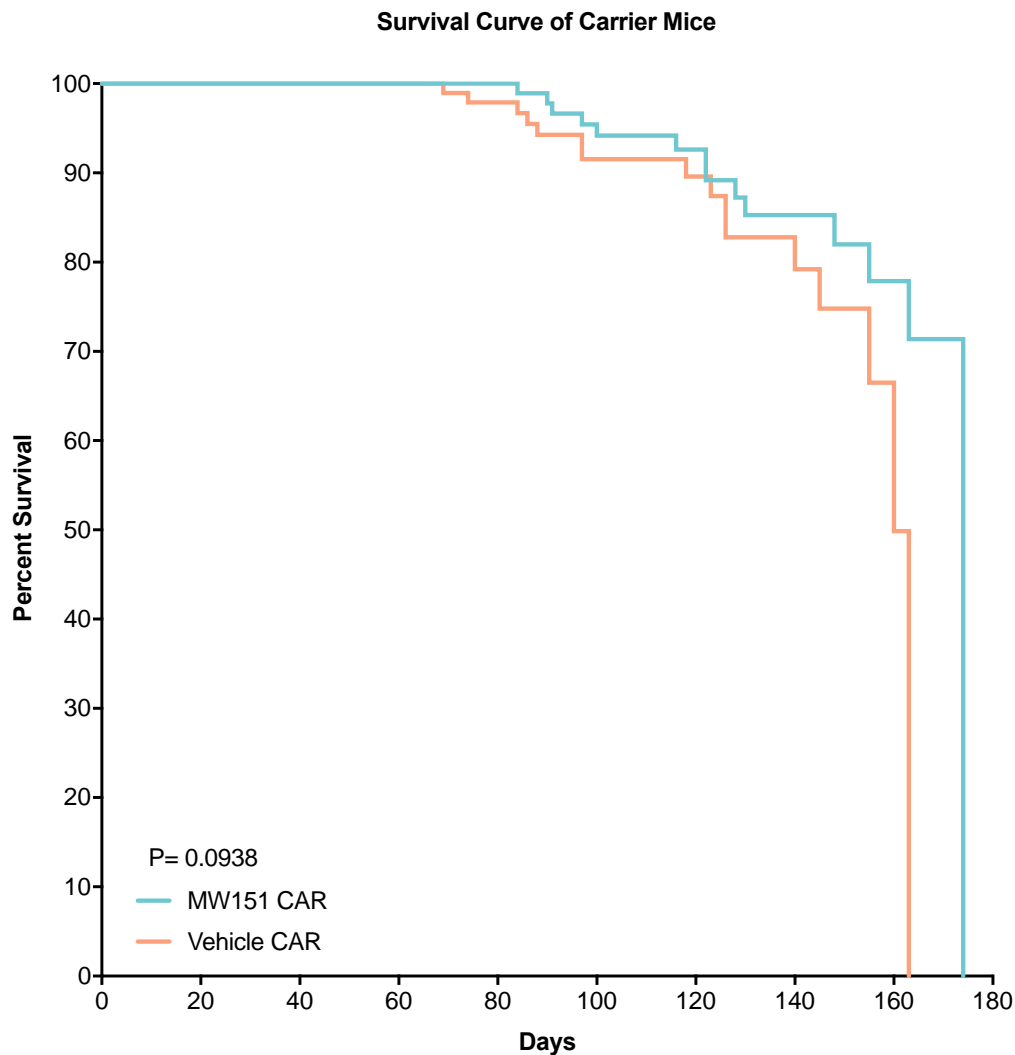


Figure 10. Life survival curve of the R6/2 mice treated with MW151 and saline. Mean lifespan of MW151 treated mice was 175 days and mean lifespan of saline treated mice was 163 days.

MW151 treated mice become modestly more active than the saline treated group

R6/2 mice in both treatments were placed in metabolic cages in order to study their activity, water/food intake, and energy expenditure. Using MW151 should increase the amount of energy expenditure of the mouse considering that it should be alleviating the burden of gliosis and potential seizure activity. Results indicate that R6/2 mice treated with MW151 would on average move around the horizontal plane more than the R6/2 saline treated mice as shown in

Figure 11A, but neither showed much interest in using the wheel provided in the cage as shown from Figure 11B. R6/2 saline treated mice expended more energy than the R6/2 treated with MW151 which could possibly indicate that the movement increased in the horizontal plane could be from seizure activity (Figure 11C). Overall, the mice treated with MW151 showed no major recovery of motor function.

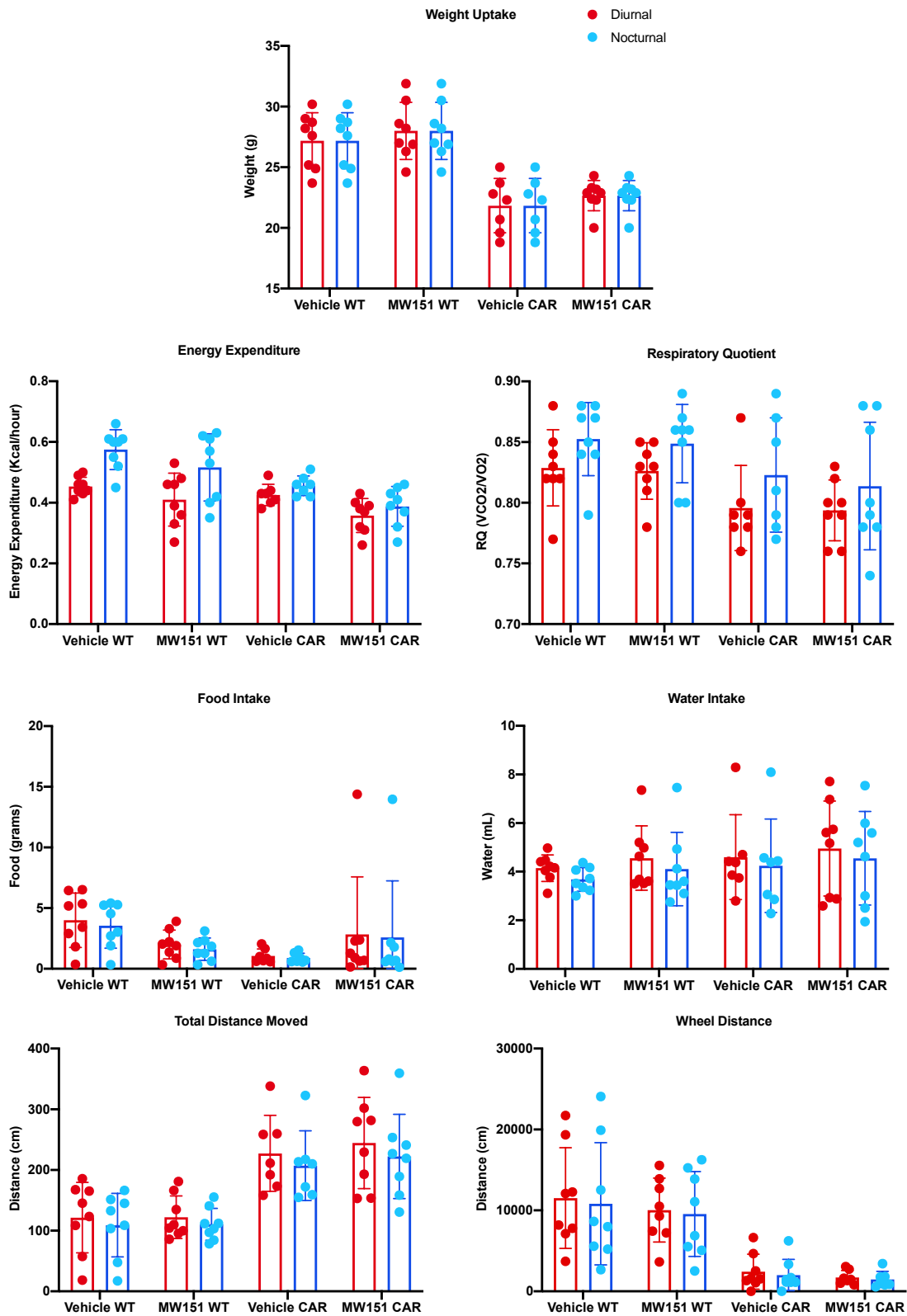


Figure 11. Metabolic cage data $N=8$ for each condition. Mice were single housed for the experiment. All mice were 10 weeks of age.

Discussion

Neuroinflammation is inflammation of the nervous system when inflicted with infections, traumatic brain injuries, toxic metabolites, or autoimmune disorders. Neuroinflammation will increase levels of systemic pro-inflammatory cytokines in order to resolve the cause of inflammation in the brain. Resident glial cells will also take a big role in neuroinflammation as their main roles are to maintain tissue homeostasis and support neurons.

Huntington's disease affects all cells in the human body and affects physiological functions in different ways. An increase in expression and transcriptional function of myeloid progenitors, PU.1 and C/EBP, in microglia cells was found in HD patients but not in normal patients (10). Lowered tolerance of stimulation from other pro-inflammatory cytokines, neuronal death, and stress of mHTT aggregates results in more active microglia. This is known as a feed forward loop. With the use of the MW151 compound we would see a decrease in pro-inflammatory mediators and a rescue in memory loss.

Our results for motor functions did not indicate a significant rescue in mobility. The rotarod and open field data indicate that the mice treated with MW151 did not show improved motor rescue. This may result from the fact that the disease is progressing much faster than the drug is aiding in rescuing the loss of neurons that relay proper motor function. However, open field data indicate that there is a minor rescue in the mice explorative behavior. This rescue can be seen in the vertical plane movements as it is known that HD mice will lose their motivation to move in both the vertical and horizontal plane.

HD mice have an average lifespan of 13-16 weeks. Mean lifespan for the HD saline treated mice was 163 days, meanwhile the mean lifespan for the MW151 treated R6/2 mice was 175. While the study shows minor changes of inflammatory mediators we also show that the

MW151 compound impacts mice lifespan expanding it by 9 days. This increase in lifespan is interesting because there was no major recovery in motor function in the mice. We anticipate the extended lifespan is due to the attenuation of weight loss or the improved heart rate. Repetition of this study would require an increase of the compound which would most likely aid in increasing the lifespan of the mice.

Memory loss in HD mice worsens as time progresses due to the loss of neurons in the striatum and cortex. In a previous study with *Webster et al.*, the team successfully aided in recovering memory function in an Alzheimer's disease model after close head injury (Webster et al., 2015). Mice would make their way through the radial arm water maze in less time than the mice that did not receive treatment. When we used the novel object recognition assay, the mice were subjected to a training phase that contained two similar objects. Mice were returned to their cages and brought back to the assay after 24 hours. The assay still contained two objects but one was novel and the other was not. Mice treated with the MW151 showed more interest in the new object and poked their nose to it more often than the old object. This led us to believe that the compound is indeed aiding in recovering memory but the effects were not as dramatic.

Minimal research has been performed to characterize the hearts of R6/2 mice. It is known that these mice have reduced heart mass and abnormal sinus rhythm. In our echocardiographs, we found that R6/2 mice hearts are significantly reduced compared to wild type. Heart rate and left ventricular mass were positively affected by the compound but did not improve cardiac output nor heart mass. While the compound is aiding in inflammation of the brain the compound does appear to affect heart and may induce more changes if applied at a higher dose.

Novel compound, MW151, is known to specifically suppress IL-1 β , TNF α , Iba1, and GFP biomarkers. In our western blot analysis, we did not detect a significant decrease in these

markers in our preliminary analysis. We are repeating this analysis and will also use ELISA assays in our future studies. This would most likely require an increase of the compound's dose which would likely lead to a more dramatic improvement in behavioral and biochemical endpoints. The compound is also known to increase synaptic protein levels and from our western blot analysis in levels of PSD95 and synaptophysin, we did not see an increase in protein levels in the MW151 treated mice compared to controls. Further analysis on the inflammatory markers is required using ELISA and possibly qPCR in order to reassess levels of protein and mRNA.

References

- An, M. C., Zhang, N., Scott, G., Montoro, D., Wittkop, T., Mooney, S., . . . Ellerby, L. M. (2012). Genetic correction of Huntington's disease phenotypes in induced pluripotent stem cells. *Cell Stem Cell*, *11*(2), 253-263. doi:10.1016/j.stem.2012.04.026
- Bachstetter, A. D., Norris, C. M., Sompol, P., Wilcock, D. M., Goulding, D., Neltner, J. H., . . . Van Eldik, L. J. (2012). Early stage drug treatment that normalizes proinflammatory cytokine production attenuates synaptic dysfunction in a mouse model that exhibits age-dependent progression of Alzheimer's disease-related pathology. *J Neurosci*, *32*(30), 10201-10210. doi:10.1523/JNEUROSCI.1496-12.2012
- Bachstetter, A. D., Zhou, Z., Rowe, R. K., Xing, B., Goulding, D. S., Conley, A. N., . . . Van Eldik, L. J. (2016). MW151 Inhibited IL-1beta Levels after Traumatic Brain Injury with No Effect on Microglia Physiological Responses. *PLoS One*, *11*(2), e0149451. doi:10.1371/journal.pone.0149451
- Becker, D. P., Barta, T. E., Bedell, L. J., Boehm, T. L., Bond, B. R., Carroll, J., . . . Yao, J. (2010). Orally active MMP-1 sparing alpha-tetrahydropyranyl and alpha-piperidinyl sulfone matrix metalloproteinase (MMP) inhibitors with efficacy in cancer, arthritis, and cardiovascular disease. *J Med Chem*, *53*(18), 6653-6680. doi:10.1021/jm100669j
- Castellano, J. M., Mosher, K. I., Abbey, R. J., McBride, A. A., James, M. L., Berdnik, D., . . . Wyss-Coray, T. (2017). Human umbilical cord plasma proteins revitalize hippocampal function in aged mice. *Nature*, *544*(7651), 488-492. doi:10.1038/nature22067
- Crotti, A., & Glass, C. K. (2015). The choreography of neuroinflammation in Huntington's disease. *Trends Immunol*, *36*(6), 364-373. doi:10.1016/j.it.2015.04.007

- Davies, S. W., Turmaine, M., Cozens, B. A., DiFiglia, M., Sharp, A. H., Ross, C. A., . . . Bates, G. P. (1997). Formation of neuronal intranuclear inclusions underlies the neurological dysfunction in mice transgenic for the HD mutation. *Cell*, *90*(3), 537-548.
doi:10.1016/s0092-8674(00)80513-9
- Egeblad, M., & Werb, Z. (2002). New functions for the matrix metalloproteinases in cancer progression. *Nat Rev Cancer*, *2*(3), 161-174. doi:10.1038/nrc745
- Gafni, J., & Ellerby, L. M. (2002). Calpain activation in Huntington's disease. *J Neurosci*, *22*(12), 4842-4849. Retrieved from <https://www.ncbi.nlm.nih.gov/pubmed/12077181>
- Gafni, J., Papanikolaou, T., Degiacomo, F., Holcomb, J., Chen, S., Menalled, L., . . . Ellerby, L. M. (2012). Caspase-6 activity in a BACHD mouse modulates steady-state levels of mutant huntingtin protein but is not necessary for production of a 586 amino acid proteolytic fragment. *J Neurosci*, *32*(22), 7454-7465. doi:10.1523/JNEUROSCI.6379-11.2012
- Graham, R. K., Deng, Y., Slow, E. J., Haigh, B., Bissada, N., Lu, G., . . . Hayden, M. R. (2006). Cleavage at the caspase-6 site is required for neuronal dysfunction and degeneration due to mutant huntingtin. *Cell*, *125*(6), 1179-1191. doi:10.1016/j.cell.2006.04.026
- Hermel, E., Gafni, J., Propp, S. S., Leavitt, B. R., Wellington, C. L., Young, J. E., . . . Ellerby, L. M. (2004). Specific caspase interactions and amplification are involved in selective neuronal vulnerability in Huntington's disease. *Cell Death Differ*, *11*(4), 424-438.
doi:10.1038/sj.cdd.4401358
- Hu, W., Ralay Ranaivo, H., Roy, S. M., Behanna, H. A., Wing, L. K., Munoz, L., . . . Watterson, D. M. (2007). Development of a novel therapeutic suppressor of brain proinflammatory

cytokine up-regulation that attenuates synaptic dysfunction and behavioral deficits.

Bioorg Med Chem Lett, 17(2), 414-418. doi:10.1016/j.bmcl.2006.10.028

Kemp, P. J., Rushton, D. J., Yarova, P. L., Schnell, C., Geater, C., Hancock, J. M., . . .

Telezhkin, V. (2016). Improving and accelerating the differentiation and functional maturation of human stem cell-derived neurons: role of extracellular calcium and GABA.

J Physiol, 594(22), 6583-6594. doi:10.1113/JP270655

Landles, C., Sathasivam, K., Weiss, A., Woodman, B., Moffitt, H., Finkbeiner, S., . . . Bates, G.

P. (2010). Proteolysis of mutant huntingtin produces an exon 1 fragment that accumulates as an aggregated protein in neuronal nuclei in Huntington disease. *J Biol Chem*, 285(12),

8808-8823. doi:10.1074/jbc.M109.075028

Li, K., Tay, F. R., & Yiu, C. K. Y. (2020). The past, present and future perspectives of matrix

metalloproteinase inhibitors. *Pharmacol Ther*, 207, 107465.

doi:10.1016/j.pharmthera.2019.107465

Lieberman, A. P., Shakkottai, V. G., & Albin, R. L. (2019). Polyglutamine Repeats in

Neurodegenerative Diseases. *Annu Rev Pathol*, 14, 1-27. doi:10.1146/annurev-

pathmechdis-012418-012857

Madushani, K. L. (2018). *Preclinical Evaluation of Matrix Metalloproteinase Inhibitors and*

Protein Kinase C Activators in Cell and Mouse Models of Huntington's Disease. (Masters of Science). Dominican University of California, Dominican University of California.

Mangiarini, L., Sathasivam, K., Seller, M., Cozens, B., Harper, A., Hetherington, C., . . . Bates,

G. P. (1996). Exon 1 of the HD gene with an expanded CAG repeat is sufficient to cause a progressive neurological phenotype in transgenic mice. *Cell*, 87(3), 493-506.

doi:10.1016/s0092-8674(00)81369-0

- Mihm, M. J., Amann, D. M., Schanbacher, B. L., Altschuld, R. A., Bauer, J. A., & Hoyt, K. R. (2007). Cardiac dysfunction in the R6/2 mouse model of Huntington's disease. *Neurobiol Dis*, 25(2), 297-308. doi:10.1016/j.nbd.2006.09.016
- Miller, J. P., Holcomb, J., Al-Ramahi, I., de Haro, M., Gafni, J., Zhang, N., . . . Ellerby, L. M. (2010). Matrix metalloproteinases are modifiers of huntingtin proteolysis and toxicity in Huntington's disease. *Neuron*, 67(2), 199-212. doi:10.1016/j.neuron.2010.06.021
- Naphade, S., Embusch, A., Madushani, K. L., Ring, K. L., & Ellerby, L. M. (2017). Altered Expression of Matrix Metalloproteinases and Their Endogenous Inhibitors in a Human Isogenic Stem Cell Model of Huntington's Disease. *Front Neurosci*, 11, 736. doi:10.3389/fnins.2017.00736
- Pido-Lopez, J., Tanudjojo, B., Farag, S., Bondulich, M. K., Andre, R., Tabrizi, S. J., & Bates, G. P. (2019). Inhibition of tumour necrosis factor alpha in the R6/2 mouse model of Huntington's disease by etanercept treatment. *Sci Rep*, 9(1), 7202. doi:10.1038/s41598-019-43627-3
- Pittayapruek, P., Meephanan, J., Prapapan, O., Komine, M., & Ohtsuki, M. (2016). Role of Matrix Metalloproteinases in Photoaging and Photocarcinogenesis. *Int J Mol Sci*, 17(6). doi:10.3390/ijms17060868
- Ring, K. L., An, M. C., Zhang, N., O'Brien, R. N., Ramos, E. M., Gao, F., . . . Ellerby, L. M. (2015). Genomic Analysis Reveals Disruption of Striatal Neuronal Development and Therapeutic Targets in Human Huntington's Disease Neural Stem Cells. *Stem Cell Reports*, 5(6), 1023-1038. doi:10.1016/j.stemcr.2015.11.005
- Rivera, S. (2019). Metalloproteinases in nervous system function and pathology: introduction. *Cell Mol Life Sci*, 76(16), 3051-3053. doi:10.1007/s00018-019-03172-8

- Rivera, S., Garcia-Gonzalez, L., Khrestchatisky, M., & Baranger, K. (2019). Metalloproteinases and their tissue inhibitors in Alzheimer's disease and other neurodegenerative disorders. *Cell Mol Life Sci*, 76(16), 3167-3191. doi:10.1007/s00018-019-03178-2
- Rocha, N. P., Ribeiro, F. M., Furr-Stimming, E., & Teixeira, A. L. (2016). Neuroimmunology of Huntington's Disease: Revisiting Evidence from Human Studies. *Mediators Inflamm*, 2016, 8653132. doi:10.1155/2016/8653132
- Saudou, F., & Humbert, S. (2016). The Biology of Huntingtin. *Neuron*, 89(5), 910-926. doi:10.1016/j.neuron.2016.02.003
- Schilling, B., Gafni, J., Torcassi, C., Cong, X., Row, R. H., LaFevre-Bernt, M. A., . . . Ellerby, L. M. (2006). Huntingtin phosphorylation sites mapped by mass spectrometry. Modulation of cleavage and toxicity. *J Biol Chem*, 281(33), 23686-23697. doi:10.1074/jbc.M513507200
- Tanaka, Y., Igarashi, S., Nakamura, M., Gafni, J., Torcassi, C., Schilling, G., . . . Ellerby, L. M. (2006). Progressive phenotype and nuclear accumulation of an amino-terminal cleavage fragment in a transgenic mouse model with inducible expression of full-length mutant huntingtin. *Neurobiol Dis*, 21(2), 381-391. doi:10.1016/j.nbd.2005.07.014
- Van Eldik, L. J., Sawaki, L., Bowen, K., Laskowitz, D. T., Noveck, R. J., Hauser, B., . . . Guptill, J. T. (2020). First-in-Human Studies of MW01-6-189WH, a Brain-Penetrant, Antineuroinflammatory Small-Molecule Drug Candidate: Phase 1 Safety, Tolerability, Pharmacokinetic, and Pharmacodynamic Studies in Healthy Adult Volunteers. *Clin Pharmacol Drug Dev*. doi:10.1002/cpdd.795
- Webster, S. J., Van Eldik, L. J., Watterson, D. M., & Bachstetter, A. D. (2015). Closed head injury in an age-related Alzheimer mouse model leads to an altered neuroinflammatory

response and persistent cognitive impairment. *J Neurosci*, 35(16), 6554-6569.

doi:10.1523/JNEUROSCI.0291-15.2015